AFGWC TECHNICAL MEMORANDUM 70-5

AFGWC

AFGWC BOUNDARY LAYER MODEL

BY
LT COL KENNETH D. HADEEN
1 APRIL 1970

PUBLISHED BY
AIR FORCE GLOBAL WEATHER CENTRAL
AIR WEATHER SERVICE (MAC)
OFFUTT AFB NEBR. 68113

DISCLAIMER NOTICE

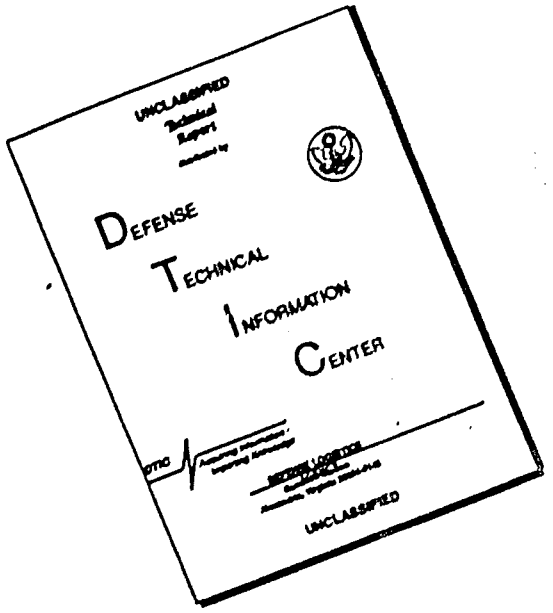

THIS DOCUMENT IS BEST QUALITY AVAILABLE. THE COPY FURNISHED TO DTIC CONTAINED A SIGNIFICANT NUMBER OF PAGES WHICH DO NOT REPRODUCE LEGIBLY.

AFGWC TECHNICAL MEMORANDA

The Air Force Global Weather Central (AFGWC) is an operational unit of Headquarters, Air Weather Service (AWS), a sub-command of the Military Airlift Command, (MAC). The AFGWC provides environmental data to the USAF, the U.S. Army, and other selected DoD units. These memoranda are brief descriptions of techniques developed by AFGWC personnel to meet military requirements. They provide detailed information on the scientific and computational methods employed. These memoranda are often preliminary in nature and are authorized by AWSR 80-2. They provide information needed by the users of AFGWC products and are for the information of other personnel conducting similar research or developmental work. Copies are available to military units and to non-military units associated with DoD activities. Other organizations may obtain copies through the Defense Documentation Center (DDC). DDC accession numbers (AD) are shown where known.

AFGWCTM 69-1 A DATA SELECTION PROCEDURE FOR THE RECTIFICATION AND MAPPING OF DIGITIZED DATA, Major Richard C. Roth, Dec 69 20 pages, AD 701374.

AFGWCTM 69-2 AFGWC FINE-MESH UPPER AIR ANALYSIS MODEL, Capt Rex J. Fleming, Dec 69, 14 pages.

AFGWCTM 69-3 DEVIATION ANALYSIS, Capt Phillip W. West, Dec 69, 13 pages, (In preparation).

AFGWCTM 69-4 EVALUATING PROBABILITY FORECASTS, Major James S. Kennedy and Capt Preston G. Epperson, Dec 69, 8 pages, AD 701375.

AFGWCTM 69-5 TROPICAL WIND AND TEMPERATURE ANALYSIS, Major August L. Shumbera, Jr., 22 Dec 69, 14 pages, AD 702449.

AFGWCTM 70-1 THE AFGWC MESO-SCALE PREDICTION MODEL, Captain James Kerlin, 22 Dec 69, 14 pages, AD 709367

(continued inside back cover)

ABSTRACT

A limited area seven layer physical-numerical model for the lower tropospheric region (surface-1600m) is described. The grid interval is half that of the standard numerical weather prediction grid used in the hemispheric, free atmospheric, operational model at the Air Force Global Weather Central (AFGWC). This model is an integral part of the complete AFGWC meso-scale (sub-synoptic) numerical analysis and prediction system. This model provides greater horizontal and vertical resolution in both the numerical analyses and numerical forecasts. It is used to predict the more detailed smaller scale atmospheric perturbations which are important in specifying sensible weather elements.

Important features of this boundary layer model include: a completely automated objective numerical analysis of input data; the transport of heat and moisture by three dimensional wind flow (including terrain and frictionally induced vertical motions); latent heat exchange in water substance phase changes; and eddy flux of heat and water vapor.

Input data are conventional synoptic surface and upper air reports. Other prediction models provide horizontal wind components at the upper boundary and an estimate of cloudiness above the boundary layer region. Forecasts for the lower boundary and surface layer are empirically derived. Despite some approximations which broadly simplify the real planetary boundary layer processes, operational use indicates the model is capable of producing detailed forecasts out to 24 hours. A winter case study is discussed.

DISTRIBUTION

Hq AWS.....6
USAFETAC.....2
AWS Wings.....2
AWS Sqdns.....2
Special

TABLE OF CONTENTS

LIST OF FIGURES

1. INTRODUCTION

This memorandum describes the Boundary Layer Model being used by the Air Force Global Weather Central (AFGWC) to produce automated forecasts of temperature, specific humidity and three dimensional wind flow in the lower 1600 meters of the troposphere. This model has been in operational production since March, 1969.

The material is presented in five sections. First, some background information is presented to place the model in perspective as to its development and integration into the AFGWC system. Next, a mathematical and physical description of the model is given. Third, the procedures used to obtain initial and forecast boundary conditions are presented. Fourth, a description of the computational model is presented, and, finally, a case study is shown.

There were several important factors which acted as guiding or limiting influences on the development of this model. The need for an operational model which would treat the thermo-hydrodyamic processes in the planetary boundary layer has existed for many years. Any model which would handle the strong horizontal and vertical gradients over highly variable terrain with appropriate consideration of adiabatic and diabatic influences as well as moisture sources and sinks must necessarily be very complex; thus, computer size and speed became important in determining the mathematical sophistication of the boundary layer model as well as the size of the forecast region. The availability of adequate data samplings required to form initial conditions for the partial differential equations which define the model also had an ex-

tremely important influence upon the model's development (especially upon the choice of grid size).

A "window" concept using a fine mesh grid has been in existence at AFGWC for several years. This system uses a detailed numerical analysis over a subregion or limited area of high operational interest. The AFGWC Fine-Mesh Upper Air Analysis Model (reference 1) uses a grid interval of approximately 100 nautical miles, or one-half the standard AFGWC Northern Hemispheric grid spacing. This analysis increases the resolution to a point where initial identification can be made of those smaller scale perturbations so important to the forecasting of sensible weather elements. The AFGWC Meso-Scale Prediction Model (reference 2) is used to provide free atmospheric forecasts of up to 24 hours over this "window area".

There are numerous theoretical boundary layer models which have been used experimentally to treat boundary layer phenomena, i.e., sea breeze, slope winds, etc. These models are usually restricted by the availability of input data, computer running time, or their inability to converge to a stable solution. The AFGWC Boundary Layer Model is the first known operational model to systematically treat many thermo-hydrodynamical interactions occurring in the atmospheric boundary layer.

Many approximations had to be made to achieve an operational model. Some of these approximations are very simple, but the ability of this model to simulate and predict, with reasonable accuracy, the behavior of the atmosphere in the boundary layer region appears to justify their use. Discussions of those approximations will be given as various aspects of the model are described.

The AFGWC Boundary Layer Model has evolved from Gerrity's (references 8 and 9) Numerical Model for the Prediction of Synoptic-scale Low Cloudiness, which was developed under USAF contract. The emphasis was changed from prediction of low cloudiness to the prediction of the basic meteorological parameters of temperature, moisture and three dimensional wind flow. Initial analyses and forecasts of these parameters provide a forecaster with the basic ingredients not only for forecasts of trends of low cloudiness, but also for the prognosis of triggering mechanisms for severe weather, low level mechanical turbulence, inversion layers (for the specification of refractive index), haze layers and many other derived meteorological parameters.

The model is designed and programmed to use the AFGWC Fine-Mesh analysis as the first guess. The model uses the wind forecasts of the AFGWC Meso-Scale Prediction Model for upper boundary conditions. An important feature of the model design is the allowance of systematic investigation of the boundary layer processes and continued development. More sophisticated techniques will be introduced into the model as more is learned about the real atmosphere within the boundary layer and those physical processes which couple the micrometeorological and synoptic scales.

2. DESCRIPTION OF THE MODEL

The AFGWC Boundary Layer Model is a hybrid which uses diagnostic techniques to obtain fields of motion and forecast techniques to solve the tendency equations for temperature and moisture. The momentum equations were not included in the model because the large horizontal and vertical gradients and the smaller scale perturbations found near the earth's surface are inadequately described by observed data. The increased computer core and computing time necessary to solve the momentum equations were not warranted without some assurance that this procedure would provide better wind forecasts than could be obtained through the diagnostic procedures. The diagnostic procedures of this model make optimum use of the output of proven free atmospheric numerical models to provide horizontal wind flow at the upper boundary. The horizontal wind at each lower level is obtained by using the detailed thermal structure of the boundary layer, geophysical parameters valid at fixed geographical locations and computed frictional forces required to obtain a resultant balanced flow.

The mathematical formulation of the model will be presented by giving the canonical form of the tendency equations for temperature and moisture, and showing how values are obtained for each term. These equations are not unique; derivations may be found in references 6 and 11. The tendency equations for temperature, specific humidity and specific moisture are:

$$\frac{\partial T}{\partial t} = -u\frac{\partial T}{\partial x} - v\frac{\partial T}{\partial y} - w\left(\frac{\partial T}{\partial z} + \frac{g}{C_p}\right) - \hat{w}\frac{g}{C_p}$$

$$+ \frac{\partial}{\partial z}\left(K_H \frac{\partial T}{\partial z}\right) + \left.\frac{dT}{dt}\right|_{diabatic} \qquad (2.1)$$

$$\frac{\partial Q}{\partial t} = -u\frac{\partial Q}{\partial x} - v\frac{\partial Q}{\partial y} - w\frac{\partial Q}{\partial z} + \frac{\partial}{\partial z}\left(K_V \frac{\partial Q}{\partial z}\right) - \left.\frac{dQ^*}{dt}\right| \qquad (2.2)$$

$$\frac{\partial R}{\partial t} = -u\frac{\partial R}{\partial x} - v\frac{\partial R}{\partial y} - w\frac{\partial R}{\partial z} + \frac{\partial}{\partial z}\left(K_V \frac{\partial R}{\partial z}\right) \qquad (2.3)$$

where T = temperature

u = horizontal wind component in the positive x-direction

v = horizontal wind component in the positive y-direction

w = frictionally induced vertical motion

$\hat{w}$ = terrain induced vertical motion

Q = specific humidity (vapor)

R = specific moisture (vapor plus liquid moisture)

K_H = coefficient of eddy conductivity

K_V = coefficient of eddy diffusivity

g = gravitational acceleration

C_p = specific heat at constant pressure

$*$ = differential of specific humidity due to change of state

The horizontal wind components (u, v) at each level are obtained from the solution of the following modified Ekman equations:

$$u = u_g + e^{-\alpha(z-h)} \left[\left(U - u_g^h \right) \cos \left(\alpha (z - h) \right) \right.$$

$$\left. + \left(V - v_g^h \right) \sin \left(\alpha (z - h) \right) \right] \qquad (2.4)$$

$$v = v_g + e^{-\alpha(z-h)} \left[\left(V - v_g^h \right) \cos \left(\alpha (z - h) \right) \right.$$

$$\left. + \left(U - u_g^h \right) \sin \left(\alpha (z - h) \right) \right] \qquad (2.5)$$

where u_g = geostrophic wind component in the positive x-direction

v_g = geostrophic wind component in the positive y-direction

z = height of level for which wind component is valid

h = height of the second level (50m)

U = wind component in the positive x-direction computed from surface layer relations

V = wind component in the positive y-direction computed from surface layer relations

α $\left(\frac{f}{2 K_m} \right)^{1/2}$

f = coriolis parameter

K_m = coefficient of eddy viscosity

Frictionally induced vertical motion (w) is obtained (neglecting variations of density) by integrating the continuity equation in the form:

$$\frac{\partial w}{\partial z} = -\left(\frac{\partial u}{\partial x} + \frac{\partial v}{\partial y} \right) \tag{2.6}$$

The terrain induced vertical motion $(\hat{w})$ is obtained by solving the following equation for each level:

$$\hat{w} = u \frac{\partial E}{\partial x} + v \frac{\partial E}{\partial y} \tag{2.7}$$

where E = terrain elevation.

Specific humidity (Q) is calculated from dew point temperature by using Teten's equation to obtain vapor pressure and by using a standard atmospheric profile for the applicable ambient pressure. Teten's equation for the relation between saturation vapor pressure and temperature is given by

$$e_s = 6.11 \times 10^{aT/(T+b)}$$

where T is the temperature, in degrees Celsius, a and b are constants. Over water, $a = 7.5$ and $b = 237.3$.

Specific moisture (R) is assumed to equal specific humidity at the initial time. This restriction will be relaxed after tests are run on the new AFGWC multi-layered nephanalyses and suitable relations between clouds and liquid moisture content have been established.

The exchange coefficients for temperature and moisture for each layer are computed from equations developed by Estoque (reference 6). These relate the exchange coefficients to stability, wind shear and

mixing length. A determination is made of whether free or forced convection exists, depending upon the Richardson number. The equation for forced convection ($Ri \geq -0.3$) is

$$K_V = K_H = \left| k^2 (1 + \beta Ri) \right|^2 \frac{\partial S}{\partial z} \qquad (2.8)$$

where k = von Karman's constant (0.38)

β = an empirical constant (-2.0)

S = wind speed shear through the layer

Ri = Richardson number, which is defined by

$$Ri = \frac{g}{\bar{T}} \left(\frac{\partial T}{\partial z} + \gamma \right) \left| \frac{\partial S}{\partial z} \right|^{-2} \qquad (2.9)$$

where $\bar{T}$ = is the mean temperature for the layer

γ = is the dry adiabatic lapse rate

The exchange coefficient for free convection ($Ri \leq -0.3$) can be written as

$$K_V = K_H = \alpha^2 \left(\frac{g}{T} \left| \frac{\partial T}{\partial z} + \gamma \right| \right)^{1/2} \qquad (2.10)$$

Where α = is an empirical constant (0.9).

The magnitudes of the eddy coefficients are bounded between 10^4 - 10^6 cm^2 sec^{-1}. It is anticipated that these bounds will be changed to a lower range after more testing has been accomplished. The value of the eddy visosity (K_m) is computed for the surface layer and is assumed independent of height for solution of equations (2.4) and (2.5). The exchange coefficients for heat and moisture are assumed equal and are evaluated for each layer of the model at each time step.

The horizontal wind components $(u,\ v)$ at 50m are computed from equations applicable only to the shallow layer adjacent to the earth's surface (the"contact layer"). An excellent derivation and discussion of these equations can be found in reference 9. The calculated values of u and v are functions of coriolis force, surface roughness, geostrophic wind and empirical results from Blackadar (reference 4) which determine a frictional velocity and turning angle for the contact layer.

The geostrophic wind components $(u_g,\ v_g)$ are obtained at each level by solving the equations

$$u_g = u_g^{z(8)} + \left[\frac{z(8) - z}{z(8) - z(2)} \right] \left[\left(u_g^{z(8)} - \bar{u} \right) \left(\frac{T(2) - T(8)}{T(8)} \right) - \frac{g\ T(2)}{f} \int_{z(2)}^{z(8)} \frac{\partial}{\partial y} \left(\frac{1}{T} \right) dz \right] \tag{2.11}$$

$$v_g = v_g^{z(8)} + \left[\frac{z(8) - z}{z(8) - z(2)} \right] \left[\left(v_g^{z(8)} - \bar{v} \right) \left(\frac{T(2) - T(8)}{T(8)} \right) + \frac{g\ T(2)}{f} \int_{z(2)}^{z(8)} \frac{\partial}{\partial x} \left(\frac{1}{T} \right) dz \right] \tag{2.12}$$

$$u = -\frac{g}{f} \frac{\partial h}{\partial y} \tag{2.13}$$

$$v = \frac{g}{f} \frac{\partial h}{\partial x} \tag{2.14}$$

Lower boundary conditions of temperature (T) and specific humidity (Q) are needed to solve the tendency equations (2.1), (2.2) and (2.3). The change in surface temperature at instrument shelter height is determined by the use of climatologically derived diurnal surface temperature change curves for clear skies and light winds. These diurnal curves are also used to simulate radiational cooling within the lower levels of the boundary layer. The temperature change curves are mean monthly values for each grid point (a curve for each month at each grid point). This change is then modified by the amount of cloudiness within and above the boundary layer. Advection and adiabatic changes are used to modify the diurnal temperature change. Finally, surface condensation is allowed, which results in modification of temperature through the release of latent heat. Surface specific humidity forecasts are made using advective and water substance phase changes only.

The saturation adjustments for temperature, specific humidity and specific moisture stem directly from the work of McDonald (reference 10). The technique allows condensation to occur with super saturation, and evaporation to occur when liquid moisture is present and the air is not saturated. Precipitation, either through or from the boundary layer, is not considered in the present model.

The coordinate system employed is a quasi-Cartesian system derived for a spherically shaped earth (small terms have been neglected). This particular Boundary Layer Model, which is currently used for the North American window, has a 29 x 27 grid. This grid is a subset of the North American fine-mesh window and has a grid spacing of approximately 100 nautical miles (one-half that of the standard AFGWC grid). A horizontal depiction of the forecast grid area is shown in Figure 1.

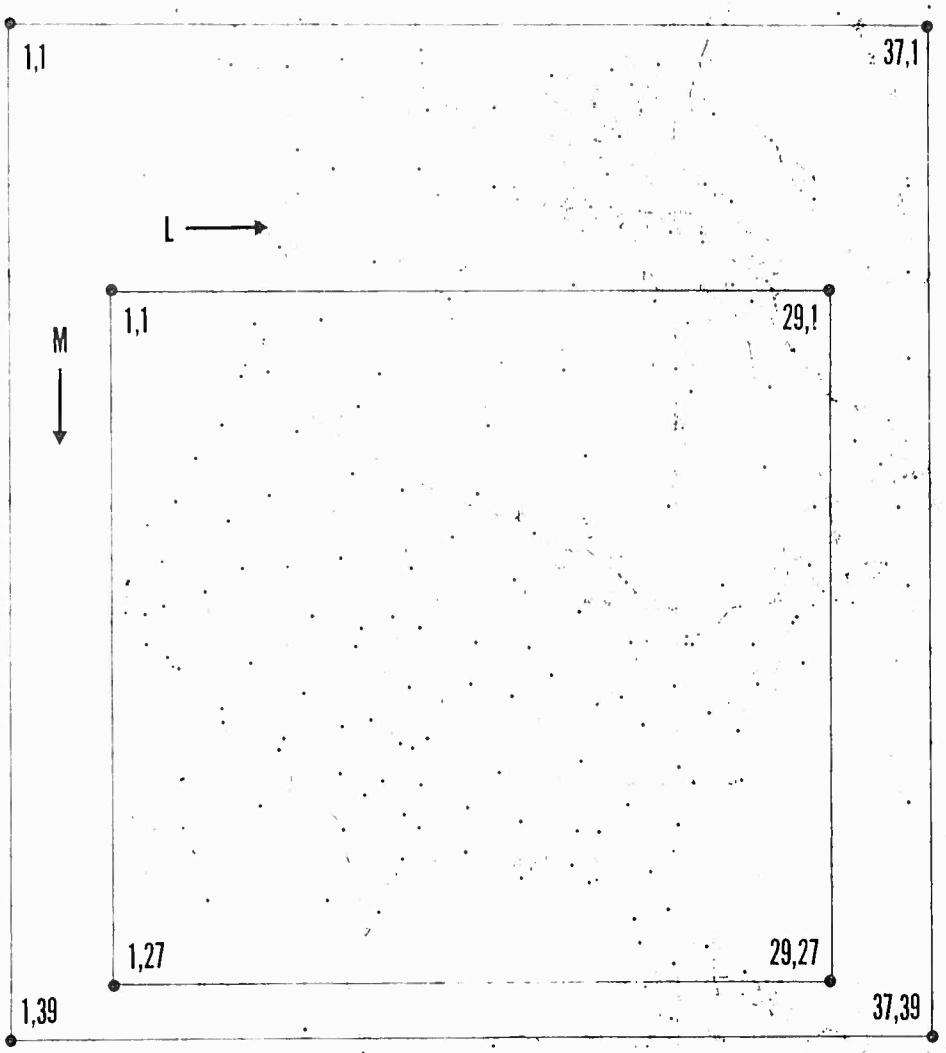

FIG. 1-HORIZONTAL DEPICTION OF AFGWC BOUNDARY LAYER MODEL

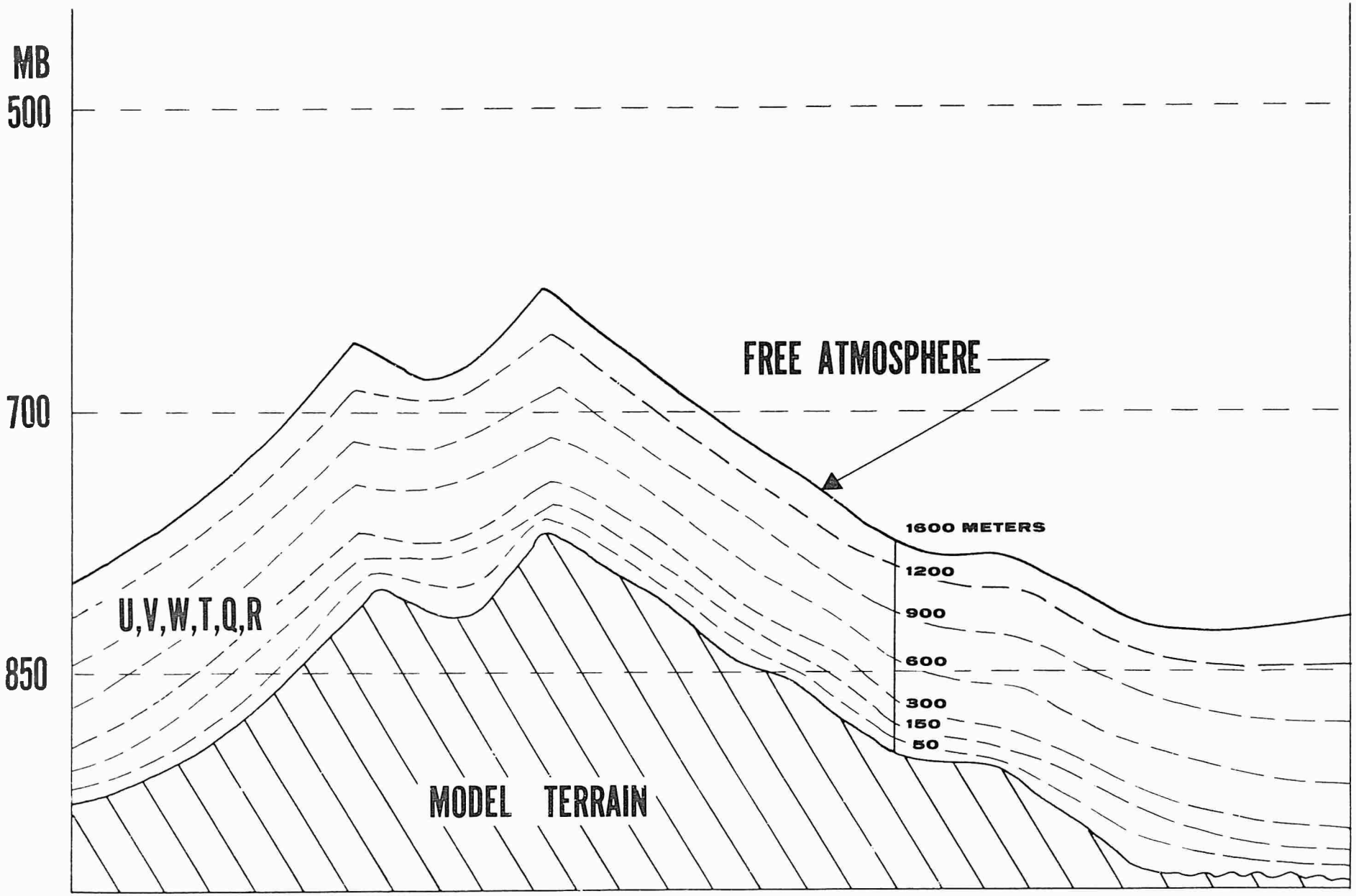

FIG. 2-VERTICAL DEPICTION OF AFGWC BOUNDARY LAYER MODEL

The inner rectangle encloses the forecast grid, and the outer rectangle encloses the boundary layer analysis grid. If we consider the grid at 80 degrees west longitude, the x-coordinate is positive to the east and the y-coordinate is positive to the north. The model includes eight levels as shown in Figure 2. The heights of the eight levels are: surface, 50, 150, 300, 600, 900, 1200, and 1600m above the surface. The vertical coordinate (z) is the height above the terrain. The fixed geometrical thickness between any two levels insures that a detailed description of the boundary layer can be obtained over variable terrain. The size of the grid, the number of levels and the thicknesses between levels can be changed easily in the operational model.

Output data for each level are stored hourly, from zero to 24 hours, in the AFGWC data base (magnetic drums). The parameters stored are the three components of the wind, temperature, D-value, geometric height, specific humidity and relative humidity.

D-values for each level are computed using output from the free atmospheric prediction model to obtain hourly forecasts of D-values at 1600m above the terrain. Values at lower levels are computed based on the specific temperature anomalies between layers.

The probability that the boundary layer model will accurately predict the future state of the atmosphere is directly related to the accuracy and representativeness of the initial and forecast boundary conditions. The next section describes in detail the techniques used in obtaining initial boundary conditions for the model equations.

3. BOUNDARY LAYER ANALYSIS

The difficulty of obtaining initial distributions of temperature and moisture which are geometrically and dynamically consistent is greater for the boundary layer region than for the free atmosphere. Factors contributing to this difficulty are: the boundary layer region is characterized by strong vertical and horizontal gradients; the finite difference technique used to solve partial differential equations requires data at fixed grid intervals, but observations are taken at arbitrary locations; surface observations may be for a height above or below the "model" terrain; the number of surface observations over the North American forecast grid is approximately ten times greater than the number of upper air observations; and most observations taken in mountainous regions are from valley reporting stations.

An automated technique was designed and programmed to provide the best possible initial numerical analyses of temperature and specific humidity with due consideration of the difficulties noted above.

The basic rationale of the analysis technique is to analyze from data dense regions toward data sparse regions. In the case of the boundary layer model, the data-dense level is at the surface and the data-sparse levels are in the region above the surface. Only conventional data, i.e., surface and upper air reports, are used in the analysis. These analyses are based on a modified Barnes technique (reference 2).

The analysis technique is data oriented; i.e., it passes through the data list to determine the data density from which an appropriate scan radius for each data point can be calculated. This radius varies from two to seven grid distances depending on data density. If there

are no data within seven grid distances, the first guess field value for the grid point in question is used in the analysis.

The boundary layer analysis programs are designed to make optimum use of data while maintaining vertical and lateral consistency. The analysis proceeds from the surface level upward to the highest level of the boundary layer model. This is accomplished by first obtaining the best possible automated surface analysis and building upward layer by layer. Analysis of lapse rates between levels rather than analysis of actual values of the parameter in the build-up procedure insures vertical consistency throughout the depth of the boundary layer.

First guess fields are obtained from the output of the AFGWC Fine-Mesh Analysis Model (reference 1). This output includes: sea level pressure, surface temperature and dew point temperature fields; temperature and specific humidity fields (calculated from dew point temperatures) at 850, 700, 500 and 300 mb. These fields are used to calculate first guess lapse rates for each layer of the model. A detailed radiosonde (RAOB) analysis for each station over the analysis region is performed to obtain data corresponding to geometric heights of each level of the model. Lapse rates of temperature and specific humidity for each layer are computed from each RAOB. This provides first guess fields and observational data for use in the analyses.

The remainder of this section will describe how the data are used.

Surface data reported in RAOBS are incorporated into the first guess surface analysis field in the following manner. Deviation data (the difference between RAOB data and the first guess analysis at the

data point location), are first computed. The value of the analysis at the data location is found by quadratic interpolation. Each deviation influences a number of grid points in the vicinity of the data. The amount of influence or weight varies with the distance between the grid point and the data point, and the scan radius computed for that data point. The weight (W) given a deviation applicable at grid point R is computed by

$$W = \exp\left\{ -4 R^2 (SR)^{-2} \right\} \qquad (3.1)$$

where R = distance from data point to grid point

SR = scan radius computed from data density

The individual contribution of each piece of deviation data at a grid point is the product of the deviation and weight computed for the data point.

Any grid point may be influenced by several pieces of data. Thus, the total change applied at a grid point is made up of normalized values of the individual changes. Each piece of deviation data contributes to the total change by an amount which is equal to the product of the deviation and the ratio of the weight for each individual data point to the sum total weight for all deviations having influence at the grid point. This method of weighting the deviation data helps to prevent the formation of unrealistically sharp gradients between sparse and dense data areas (such as sea coasts).

After the contributions of all deviations have been considered to form a change field, the first guess field and the change field are added. The resulting field is an improved estimate of the analysis

field. The deviation data are again computed from the refined analysis and the original RAOB data. The same procedures are followed to compute a new change field. The procedure is repeated three times, with each successive scan providing closer agreement between data and analysis.

The analyses of temperature and specific humidity above the surface are produced in a somewhat different manner than at the surface. The important differences lie in the method of obtaining the first guess fields for the deviation analyses and in the use of lapse rate analyses instead of actual values of the respective parameters.

The first-guess lapse rate analyses, computed from the output of the Fine-Mesh Upper Air Analysis Model, tend to be noisy, especially over variable terrain. Therefore, a certain amount of smoothing is necessary. A smooth first guess field is obtained by taking the actual RAOB lapse rate data, spreading the data to grid points, and combining the resultant field with the preliminary guess field. The actual RAOB lapse rate data are used to compute deviation data, which, in turn, are used to compute change fields in the same manner as at the surface. The first guess field is then refined by addition of the change field. This procedure is repeated three times.

The magnitude of the temperature lapse rate is limited by a value computed from the equation

$$C = \left\{ -\gamma_d - \gamma_z \frac{1}{(1 + L^2)} \right\} \Delta z \qquad (3.2)$$

where C = cut-off value (deg m^{-1})

γ_d = dry adiabatic lapse rate (0.0098 deg m^{-1})

Γ_d = autoconvective lapse rate (0.0342 deg m^{-1})

L = a parameter varying from one to L, where one is the bottom layer and L is the top layer

Δz = thickness of the layer (m)

The cut-off value rapidly approaches the dry adiabatic lapse rate as the height above the surface increases. For temperature lapse rates, the analysis at each grid point is checked against the cut-off value after each scan. If the lapse rate exceeds the cut-off value, the lapse rate is replaced with the limiting value.

Analyses of temperature and specific humidity are produced for the level at the top of each layer by adding the value of the lapse rate through the layer to the value of the parameter at the next lower level. In the specific humidity analyses, a check is made to avoid negative and supersaturated values. The analyzed values obtained for specific humidity are used as initial values of specific moisture.

4. THE COMPUTATIONAL MODEL

The previous sections in this report dealt mainly with equations used in the model and the method of analysis used to provide initial and forecast boundary conditions. This section describes the design of the computer program and the basic techniques used to solve the equations of the model.

A packed data format is used to reduce computer core requirements. The packing scheme and data ranges are given in Table 1. This packing scheme allows the use of 79 fields in core at one time (the same amount of the core would accomodate only 22 fields of unpacked data).

The tendency equations (2.1), (2.2) and (2.3) were transformed to a linearized set of finite difference equations in which the coefficients are assumed constant for a given time increment. These equations are solved by an uncentered (upstream) difference technique. A combination of a forward difference for the time derivative and upstream difference for the space derivative is used; this procedure has the advantage of remaining computationally stable as long as the standard numerical stability criterion $\Delta T \leq \frac{\Delta x}{C}$ is satisfied. Here, ΔT is the time step (30 minutes), Δx is the grid interval and C is the speed of the advecting wind plus the rate of movement of the system. From a theoretical viewpoint, the upwind difference approximation is less accurate than a centered difference approximation. However, from a practical viewpoint the upwind method is in better agreement with the physical concept of advection. In determining the time rate of change due to advection of a quantity at a given point in space and time, only the upstream values of a quantity are of importance.

[illegible]	[illegible]	[illegible]	[illegible]	[illegible]	[illegible]	[illegible]	[illegible]
[illegible]	[illegible]	[illegible]	m·sec^{-1}	[illegible]	[illegible]	[illegible]	[illegible]
[illegible]	[illegible]	[illegible] to [illegible]	m·sec^{-1}	0.1	10 [illegible]	M1 ([illegible])	10-1[illegible]
[illegible] Moisture	[illegible]	[illegible] to [illegible]	[illegible]	0.1	10 [illegible]	M1 ([illegible])	[illegible]
[illegible]	[illegible]	[illegible] to [illegible]	cm·sec^{-2}	[illegible]	10^{-4} [illegible]	M1 ([illegible])	[illegible]
Vertical Velocity	[illegible]	-12 to 12	cm·sec^{-1}	0.1	[illegible]	M2 ([illegible])	0-[illegible]
Terrain Vertical Velocity	[illegible]	-12 to 12	cm·sec^{-1}	[illegible]	10 [illegible]	M2 ([illegible])	8-1[illegible]
[illegible]	[illegible]	[illegible] to [illegible]	gm·kg^{-1}	0.1	10 [illegible]	M2 ([illegible],E)	16-24
Temperature	[illegible]	200 to 400	[illegible]	0.1	10 ([illegible]-200)	M2 ([illegible])	25-35
[illegible] Component [illegible]	[illegible]1	[illegible]	m·sec^{-1}	0.1	10 [illegible]	M1 ([illegible])	0-[illegible]
[illegible] Component [illegible]	[illegible]2	-50 to 50	m·sec^{-1}	0.1	10 [illegible]2	M1 ([illegible])	10-1[illegible]
Sfc Temperature [illegible]	[illegible]1	[illegible] to 330	[illegible]	0.1	10 [illegible]1	M1 ([illegible])	24-3[illegible]
[illegible] Component [illegible]	[illegible]1	-50 to [illegible]	m·sec^{-1}	0.1	10 [illegible]1	M2 ([illegible])	0-[illegible]
[illegible] Component [illegible]	[illegible]2	-50 to [illegible]	m·sec^{-1}	0.1	10 [illegible]2	M2 ([illegible])	10-1[illegible]
Sfc Temperature [illegible]	[illegible]2	[illegible] to 330	[illegible]	0.1	10 [illegible]2	M2 ([illegible])	24-3[illegible]
Longitude ([illegible])	[illegible]	-180 to 180	deg	0.1	10 [illegible]	M3 (L,M)	0-11
Latitude	[illegible]	[illegible] to [illegible]	deg	0.1	10 [illegible]	M3 ([illegible])	12-21
Sfc Roughness	[illegible]	0 to [illegible]00	cm	1.0	1 [illegible]	M3 (L,M)	22-30
Sfc Elevation		0 to 5000	m	10.0	10^{-1} [illegible]	M4 (L,M)	0-[illegible]
Sfc Specific Humidity	[illegible]	0 to 50	gm·kg^{-1}	1.0	10 [illegible]	M4 (L,M)	9-17
[illegible]	[illegible]	[illegible] to [illegible]	[illegible]	1.0	[illegible]	M4 ([illegible])	1[illegible]-24
Friction[illegible] Velocity	[illegible]	[illegible] to [illegible]	cm·sec^{-1}	1.0	[illegible]	M4 ([illegible])	25-34
[illegible]ndex	[illegible]	0 or [illegible]			[illegible]	M4 ([illegible])	35
[illegible] Coefficient	[illegible]	-10 to [illegible]		0.1	10 [illegible]	M5 ([illegible])	0-7
[illegible]	[illegible]	[illegible] to 10[illegible]		1.0	[illegible]	M5 ([illegible])	16-22
Sfc Temperature	[illegible]	[illegible] to 330	[illegible]	0.1	10 [illegible]	M5 ([illegible])	24-3[illegible]
[illegible] Analysis	[illegible]	1 to [illegible]		1.0	[illegible]1	M6 ([illegible])	0-8
[illegible] Forecast [illegible] Hour	[illegible]	[illegible]		1.0	[illegible]2	M6 (L,M)	9-17
[illegible] Forecast 12-18 Hour	[illegible]	[illegible] to 3		1.0	[illegible]3	M6 (L,M)	18-26
[illegible] Forecast [illegible]-24 Hour	[illegible]	1 to 3		1.0	[illegible]	M6 (L,M)	27-35
Heat Flux	[illegible]	unspecified	deg·cm·sec^{-1}	floating point	HF	HF (L,M)	0-35
[illegible] Flux	VF	unspecified	cm·sec^{-1}	floating point	VF	HF (L,M)	0-35

Certain boundary conditions are applied in the solution of the tendency equations. Outflow is allowed at the lateral boundaries of the forecast grid but inflow is not. This restriction causes a degradation of the forecast on the windward side of the boundary layer forecast region. This degradation penetrates the region with the speed of the wind. Various techniques have been investigated to remove this restriction, but no real breakthrough is anticipated until lateral boundary conditions can be forecast with higher fidelity.

The general flow of the complete model is depicted in Figure 3. The large quantity and variety of data required to prepare the initial and forecast boundary conditions, and the complexity of the forecast model require sequential operation of eight main computer programs. There are numerous subprograms associated with each of these programs. Six programs are required to pre-process and analyze the data prior to execution of the forecast program. One program is used for the prognostic model and one program is used to accomplish the post- processing and storage of selected parameters into the AFGWC drum data base.

The remainder of this section will describe the functions performed by each program. The purpose of this description is to clarify what data are used and how the model operates. The AFGWC computer system is drum oriented; temporary, immediate access, drum storage is used. The data used by the model are available in the AFGWC drum data base.

4.1 Boundary Layer Analysis Programs

The first analysis program checks the AFGWC drum data base for the presence of the data required to execute the model. If the required fields are available, a terrain elevation field is read from the data

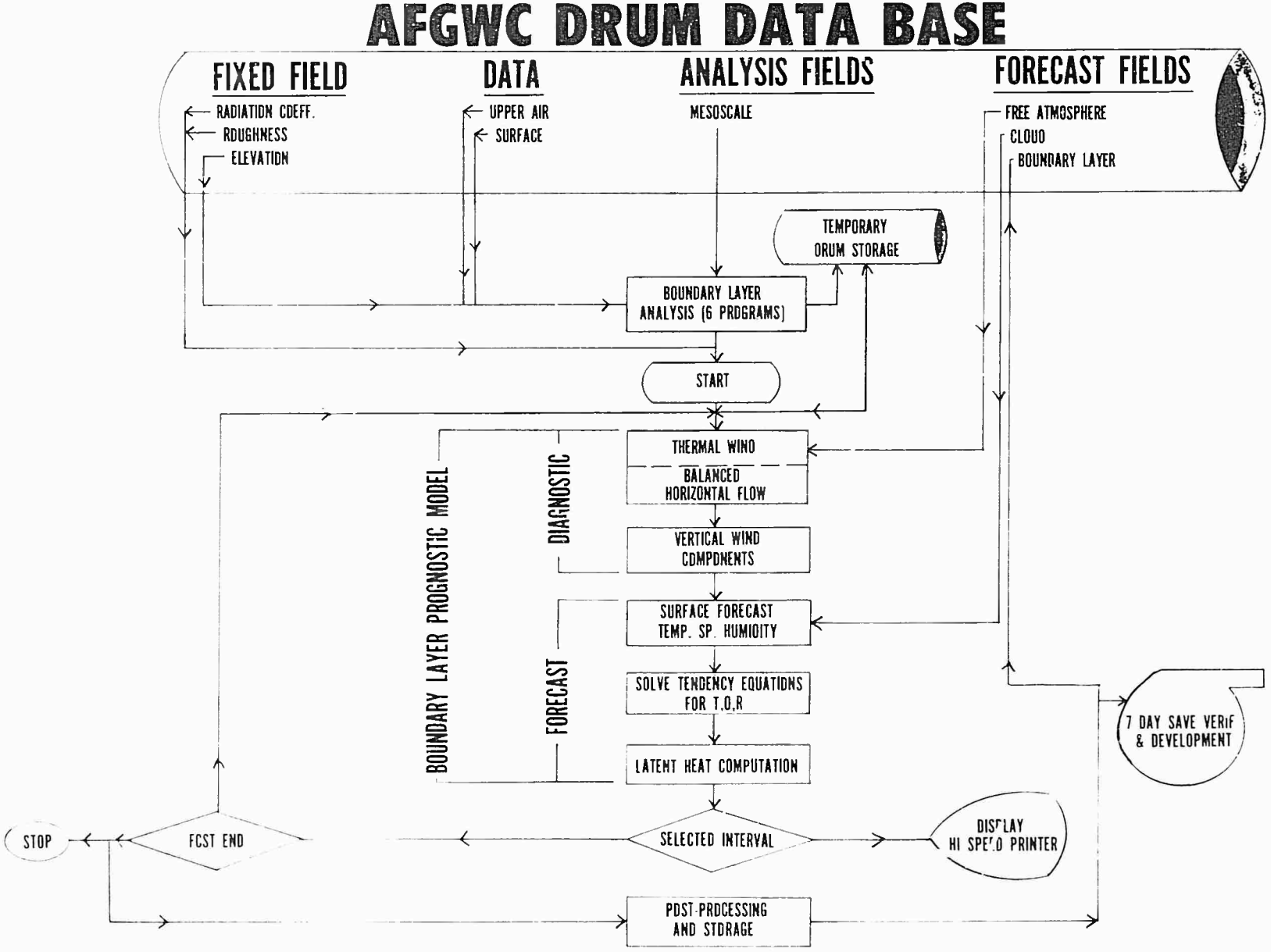

FIG.3 FLOW DIAGRAM OF OPERATIONAL BOUNDARY LAYER MODEL

base. The field applicable to the boundary layer window is extracted and written on a drum file for later use in the analysis programs.

The second analysis program reads the fine-mesh analysis fields from the drum data base and computes fields of specific humidity for the surface, 850, 700, 500, and 300 mb levels. Surface pressure, temperature and specific humidity fields for the window are written on drum for later use. Finally, this program computes temperature and specific humidity lapse rates for each layer of the model. These first guess fields are also written on a drum for later use in the analyses.

The third analysis program reads the RAOB data for the boundary layer window from the AFGWC drum data base. A hydrostatic check is made and geopotential heights for each significant level are computed using the hypsometric equation. The reported values of temperature and computed values of specific humidity for each sounding are then used to interpolate values for each model level. Finally, these values are written on drum for later use.

The fourth analysis program reads the first guess fields and RAOB data from the drum files and produces analyses of temperature and specific humidity for each level of the model.

The fifth analysis program reads the analysis fields, fixed field data (i.e. radiational coefficients, surface roughness and terrain height) and cloud data from drum files, and arranges the data in a form that can be used by the forecast program. These data are packed into the appropriate arrays. These arrays are written on drum and are ultimately read and used by the forecast model.

The sixth analysis program retrieves fine-mesh analysis and forecast fields of u and v components for the 850, 700, and 500 mb levels from the AFGWC drum data base. These fields are then used to interpolate a 1600 meter above ground level (AGL) wind analysis for the inital time and forecasts for each hour out to 24 hours. Finally, the interpolated u and v components are packed into appropriate arrays and saved on drum. At this point all data necessary to execute the prognostic phase of the boundary layer package are available on drum files in the format required by the model.

4.2 Boundary Layer Prognostic Programs

The forecast model program reads initial conditions from drum files, solves the finite difference versions of the diagnostic equations (2.11) and (2.12) and computes the geostrophic wind at each level. The finite difference versions of equations (2.4) and (2.5) are solved to obtain a balanced horizontal flow for each level. The finite difference versions of equations (2.6) and (2.7) are solved to obtain vertical velocities induced by surface friction and terrain. At this point, the model begins its prognostic cycle by forecasting the surface temperature and surface specific humidity for the next time step. The finite difference versions of the tendency equations (2.1), (2.2) and (2.3) are then solved to obtain temperature, specific humidity and specific moisture for the next forecast time. The latent heat computation and appropriate adjustments of temperature, specific humidity and specific moisture are made. The program is then ready to read in a new upper boundary wind, make a diagnosis of the flow at the remaining levels from the new forecast temperature distribution, make new surface forecasts, etc.

Selected forecast displays are output on a high speed printer for desired forecast intervals.

4.3 Post-Processing and Storage Programs

The model outputs the data listed in Table 1, at hourly forecast intervals, on a drum file. These data are packed in the arrays named in the table, using the horizontal coordinates, L and M, and the vertical coordinate, K, as subscripts identifiying the grid point and level.

The last program reads and unpacks these arrays, calculates 1600m AGL D-values from the output of the AFGWC Meso-Scale Prediction Model (reference 2), and subsequently computes relative humidities and D-values for each level of the boundary layer model. The data are then stored in the AFGWC drum data base.

The next section is a study of a representative case, showing some of the model's capabilities and samples of the available output.

5. CASE STUDY

This section is devoted to a case study for 16 January 1970. The purpose of this study is to demonstrate the detailed initial analysis, the applicability of the diagnostic wind procedures for flow over variable terrain at both initial and forecast times and to show the type of output which is routinely available from the model. The performance of the model on this particular case isn't any better or worse than can be expected on a particular day.

The general synoptic situation at 0000Z on 16 January 1970 is depicted in Figure 4 (reproductions of facsimile charts transmitted by the National Meteorological Center). The main storm track was through the Southern United States as evidenced by the occluded system approaching the West Coast, the remains of an occluded system along the New Mexico-Texas border and the wave disturbance off Southeastern Florida. Arctic and modified arctic air dominated Canada and the Northern United States. The cold arctic high over Western Canada had been nearly stationary during the previous 24 hours.

Figures 5 thru 8 show the rapid wave development and formation of an occlusion in the Great Lakes Region, the cold penetration of arctic air along the Eastern slopes of the Rocky Mountains, the development of a wave along the arctic front in Eastern Colorado and the movement of the occluded system into the Western United States.

A few streamlines have been placed on Figure 9 to show the wind flow at 1500m above the terrain. This wind field was derived from height fields from the 850, 700 and 500 mb meso-scale analyses. The diagnosed flow at 50m is shown in Figure 10. The superimposed isobaric analysis,

with fronts, highs and lows, was obtained from the analysis depicted in Figure 4. Of interest is the outflow around the highs located along the Virginia coast and over Eastern Canada, the inflow in the vicinity of the inverted trough through northern Iowa into northwestern Wisconsin and across Western Lake Superior. Flow associated with the arctic high and especially the flow in the vicinity of the 1016 mb isobar over Nevada, Idaho, Utah and Colorado

The 12 hour forecasts of winds at 1600m and 50m AGL are depicted in Figures 11 and 12, respectively. Compared with the independent verifying analysis, it is apparent that the model showed a more open wave in the Great Lakes Region with the warm frontal trough over Lake Huron and Lake Ontario. The model tended to push the cold air southward along the mountains more rapidly and eastward in Wisconsin more slowly than the verifying analysis indicated. The flow forecast in the vicinity of the high centered over the four corners area of Colorado, New Mexico, Arizona and Utah appears to be extremely accurate.

The 24 hour forecast of winds at 1600m and 50m are shown in Figures 13 and 14, respectively. It is interesting to note that the 50m wind field indicates the frontal system shown on the verifying analysis over Nevada could be nearer the Utah border (surface observations shown in Figure 8 tend to support this conclusion). The forecast of the winds associated with the leading edge of the arctic high trailed the actual frontal position by a full grid length at the end of the 24 hour forecast. The lee side trough over Eastern Colorado with the associated wave on the arctic front in the Nebraska panhandle is well represented by the boundary layer forecast.

The frontal positions from Figures 4, 6 and 8 were consolidated into a continuity chart shown in Figure 15. This figure also shows the location of grid row 11 in relation to the arctic high east of the Rocky Mountains.

The wind directions displayed in Figure 16 (a time cross-section at grid point near Medford, Oregon) are given in relation to the co-ordinate system used in the model, and it is necessary to subtract 45° from the direction to obtain wind direction in relation to true north. It is interesting to note the development of the wind max at approximately 300m above the surface during the 4-6 hr forecast period, associated with frontal passage forecast for the area. The isotherm pattern also is quite indicative of the frontal passage and shows the relatively homogenous air mass behind the front.

An entirely different situation is depicted in Figure 17, which shows a time cross-section at a grid point near Limon, Colorado (subtract 25° from all wind directions to convert to true directions). At the initial time, relatively warm air was over this grid point. Later, the arctic air over Nebraska moved southward bringing cold air over the grid point; a wave developed on the arctic boundary and the cold air receded. Westerly, down-slope winds then caused strong adabiatic warming which is in evidence at the end of the forecast period.

The eastward movement of the arctic high with the rapid occlussion of the frontal system is shown in Figures 18, 19 and 20. In these figures, the scale is greatly distorted; the vertical coordinate is approximately two miles while the abscissa is nearly 3000 miles. The call letters of stations are only approximate locations and may be either

north or south of the actual grid row.

D-values computed in the post-processing phase of the operational run have proven very useful in locating and predicting frontal movements. An interpolated D-value field at 1600m AGL is depicted in Figure 21. An analysis of the D-values computed for the surface is shown in Figure 22. Frontal positions together with high and low pressure centers (from Figure 4) were added to show correlation with the surface analysis.

The 12 hour forecast of D-values at 1600m AGL (from the free atmospheric model) is shown in Figure 23. The computed surface D-value from the forecast temperature structure is shown in Figure 24. The boundaries of the arctic air are clearly defined on this chart. Forecasters often do not realize the great change in D-value which can occur vertically in the boundary layer region. For example, note the arctic high over Western Canada where the D-value at 1600m AGL is approximately -40 feet, while at the surface the D-value is +690 feet.

Temperature soundings for two stations are shown in Figure 25. The sounding for Albany shows that in 12 hours a slightly unstable layer between 150 and 600m became a stable inversion whereas at Omaha an inversion between 300 and 600m became more unstable with the strong advection of cold air. The very strong gradients associated with an arctic out-break of this type require a very precise initial representation of the thermal structure and a very accurate forecast of winds at all levels to completely capture the forecast change.

This winter case study demonstrates the capability of the model to analyze and forecast detailed changes with considerable fidelity.

It is anticipated that further refinement of radiation coefficients and roughness fields will be made as daily evaluation of the Model continues. Further development in the area of exchange coefficients for transport of heat and moisture by eddy motion, and a more refined thermal wind computation may further improve the forecasts from this model.

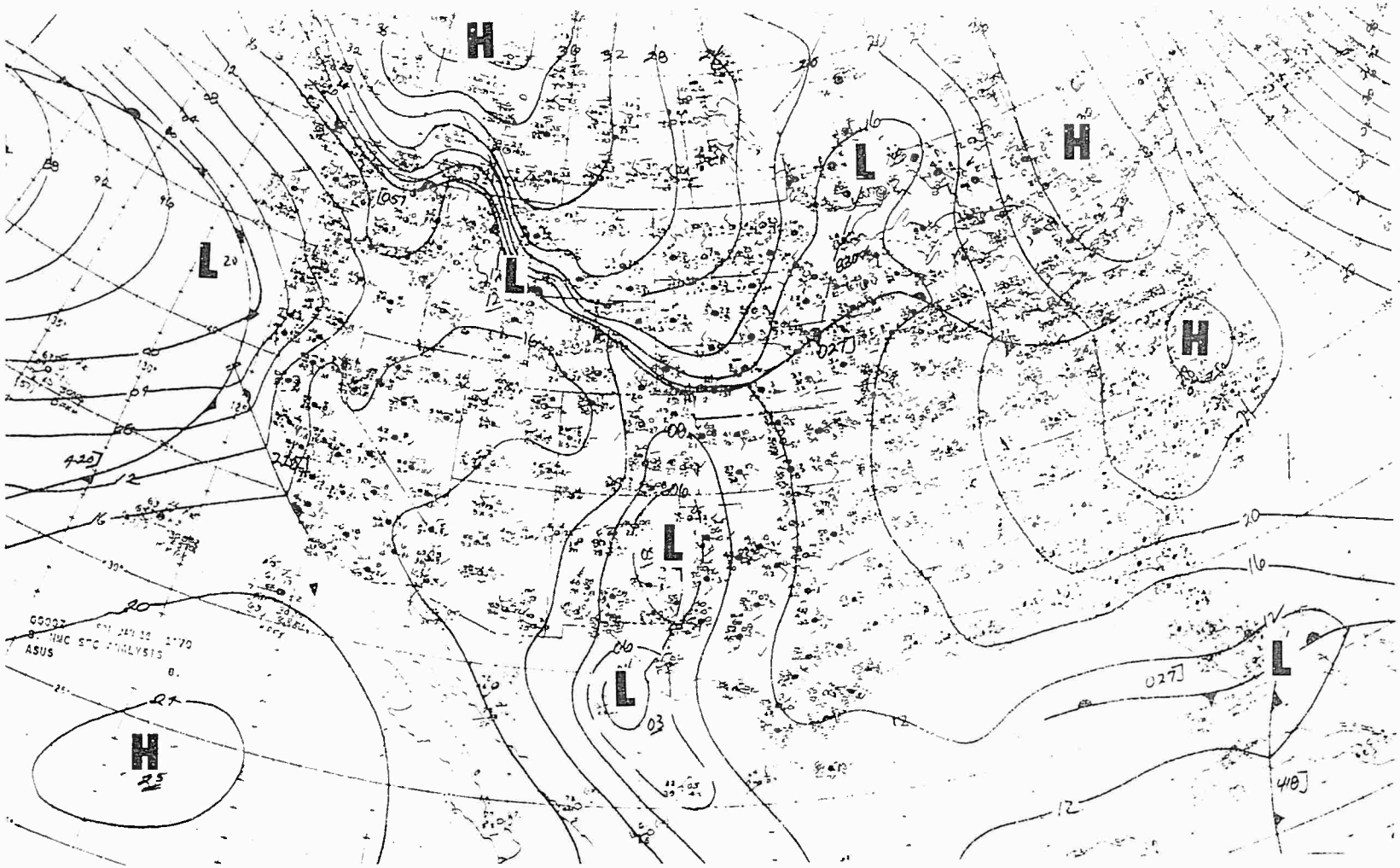

FIG. 4 SURFACE ANALYSIS FOR 0000Z 16 JANUARY 1970

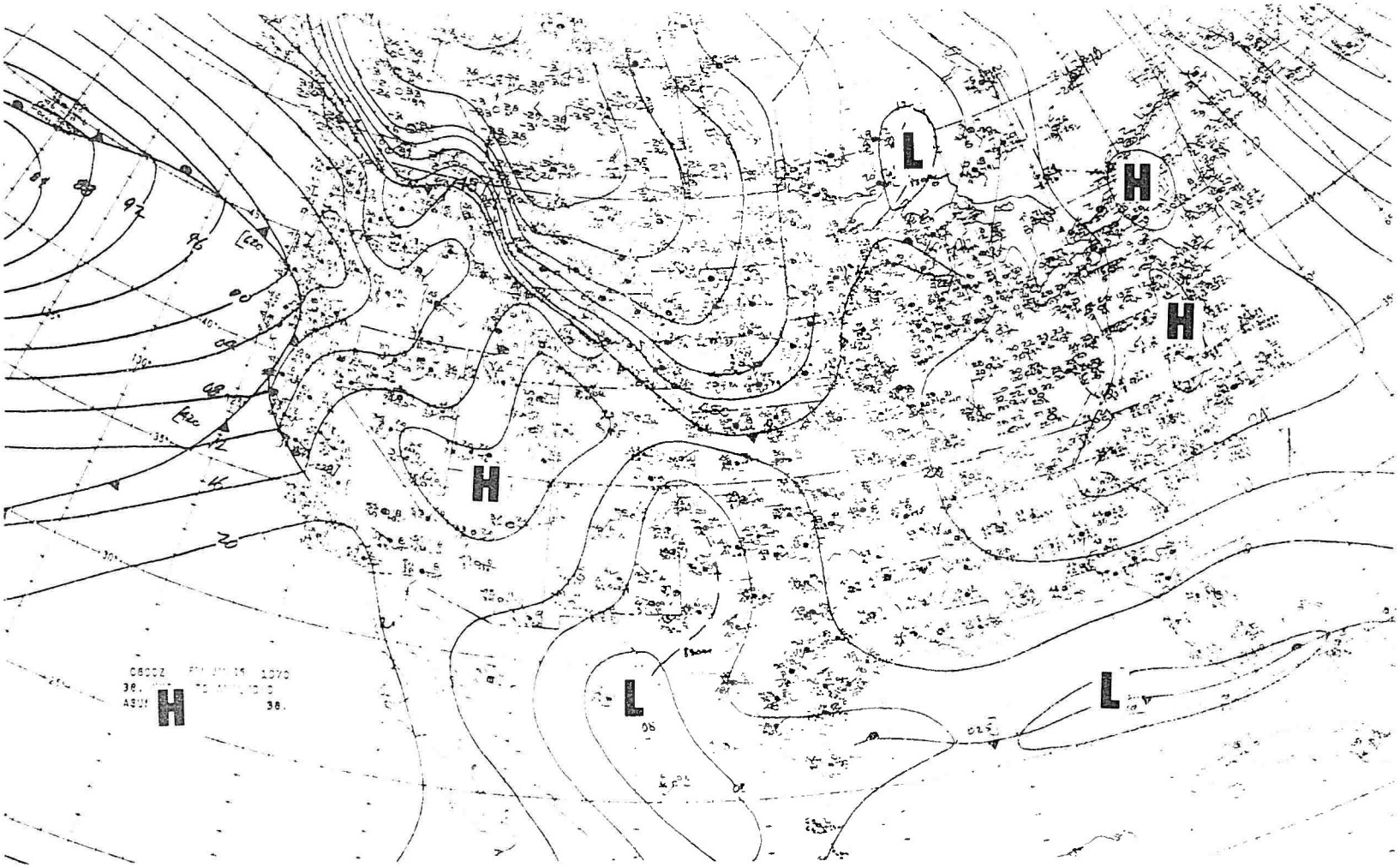

FIG. 5 SURFACE ANALYSIS FOR 0600Z 16 JANUARY 1970

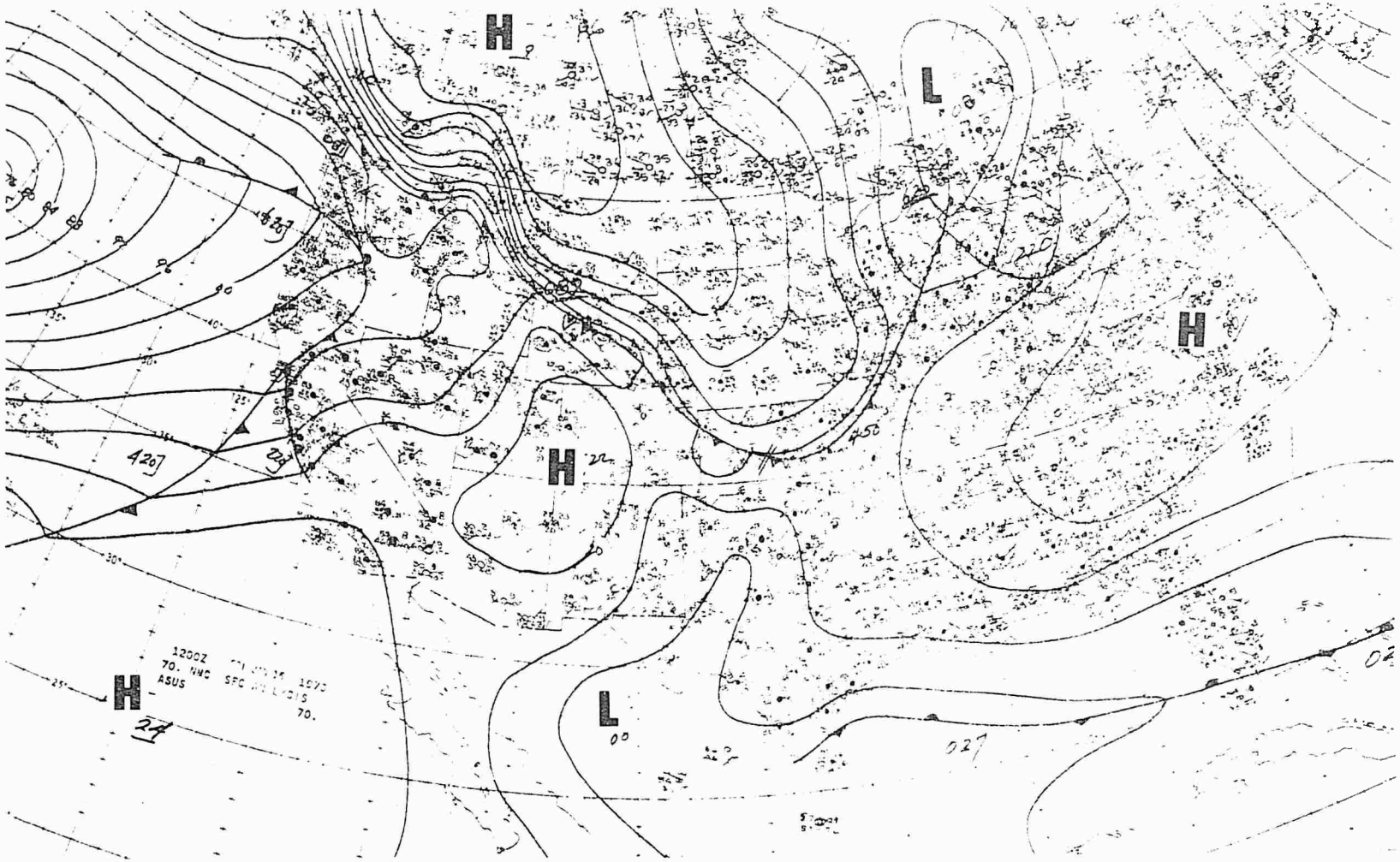

FIG. 6 SURFACE ANALYSIS FOR 1200Z 16 JANUARY 1970

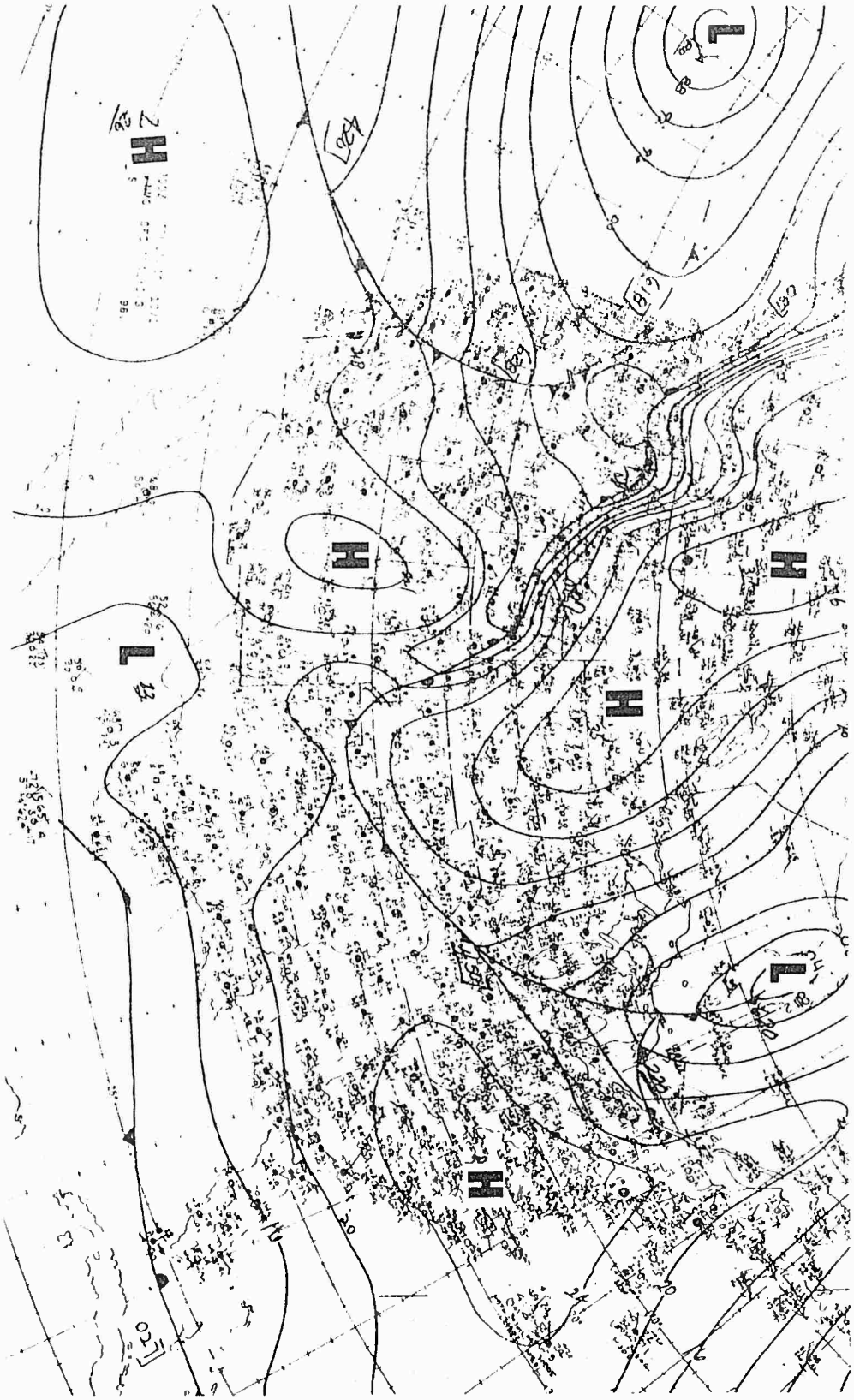

FIG. 7 SURFACE ANALYSIS FOR 1800Z 16 JANUARY 1970

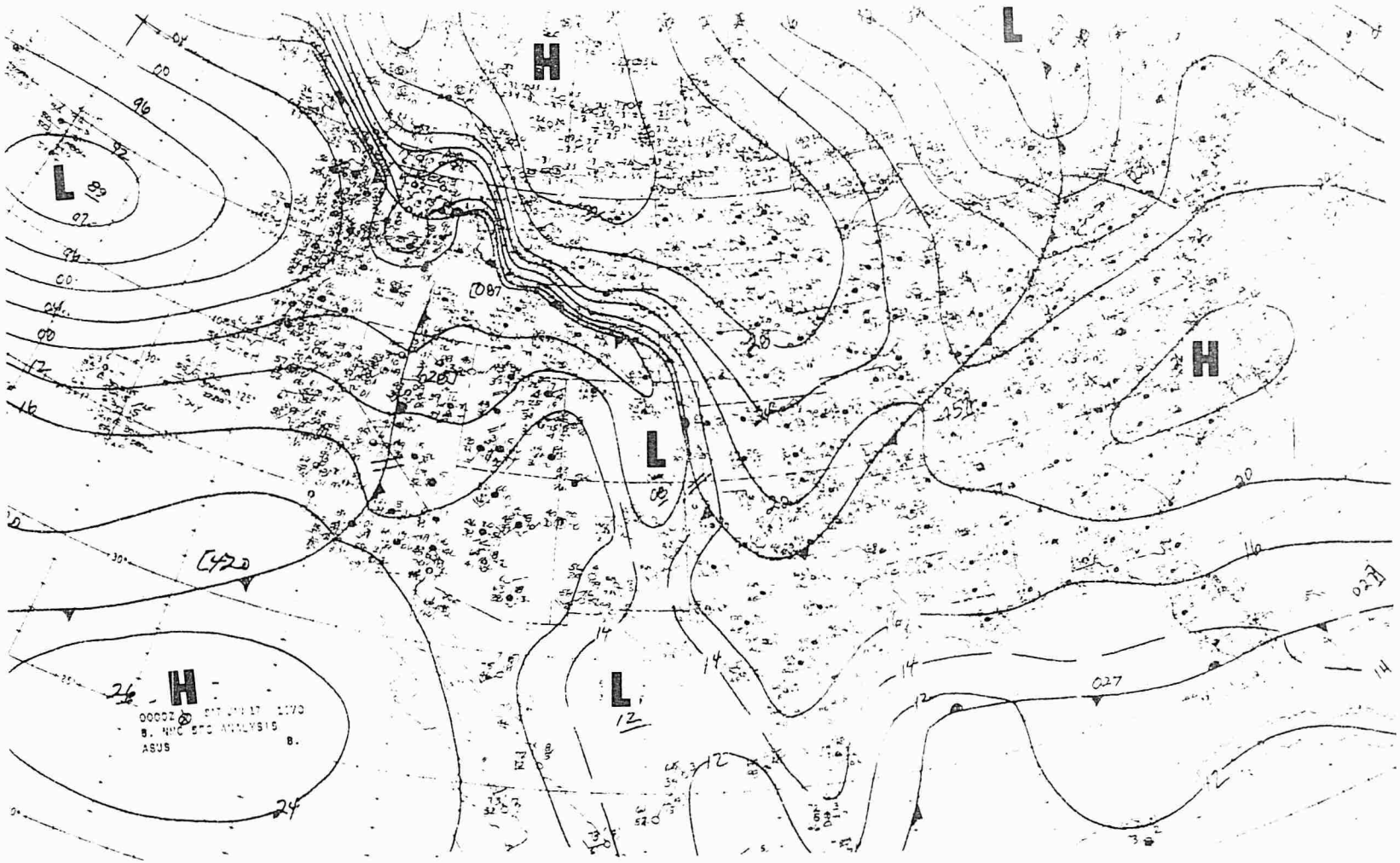

FIG. 8 SURFACE ANALYSIS FOR 0000Z 17 JANUARY 1970

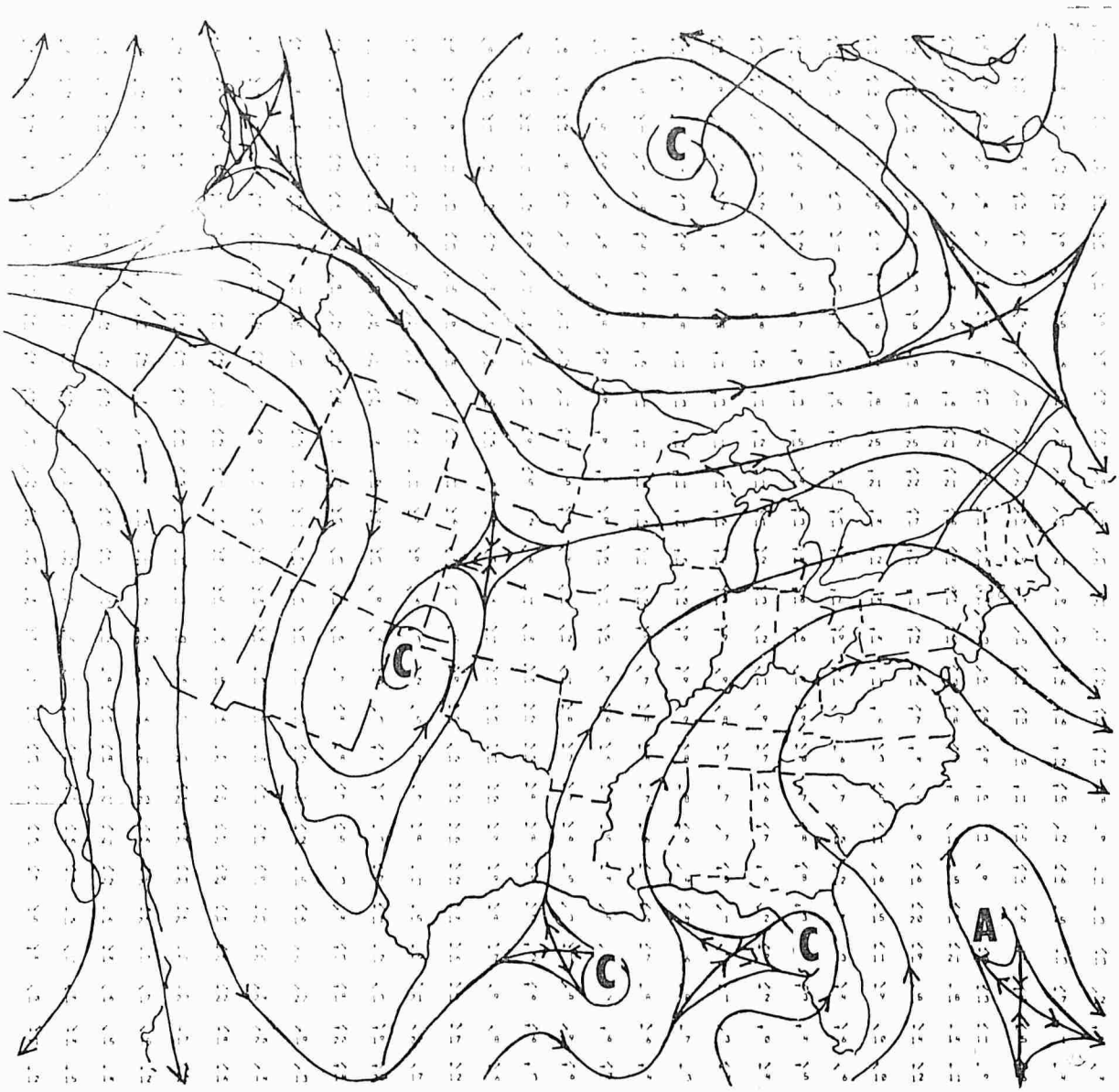

WIND SPEEDS IN METERS PER SECOND

FIG. 9 DERIVED 1600m WIND FLOW FOR 0000Z 16 JANUARY 1970

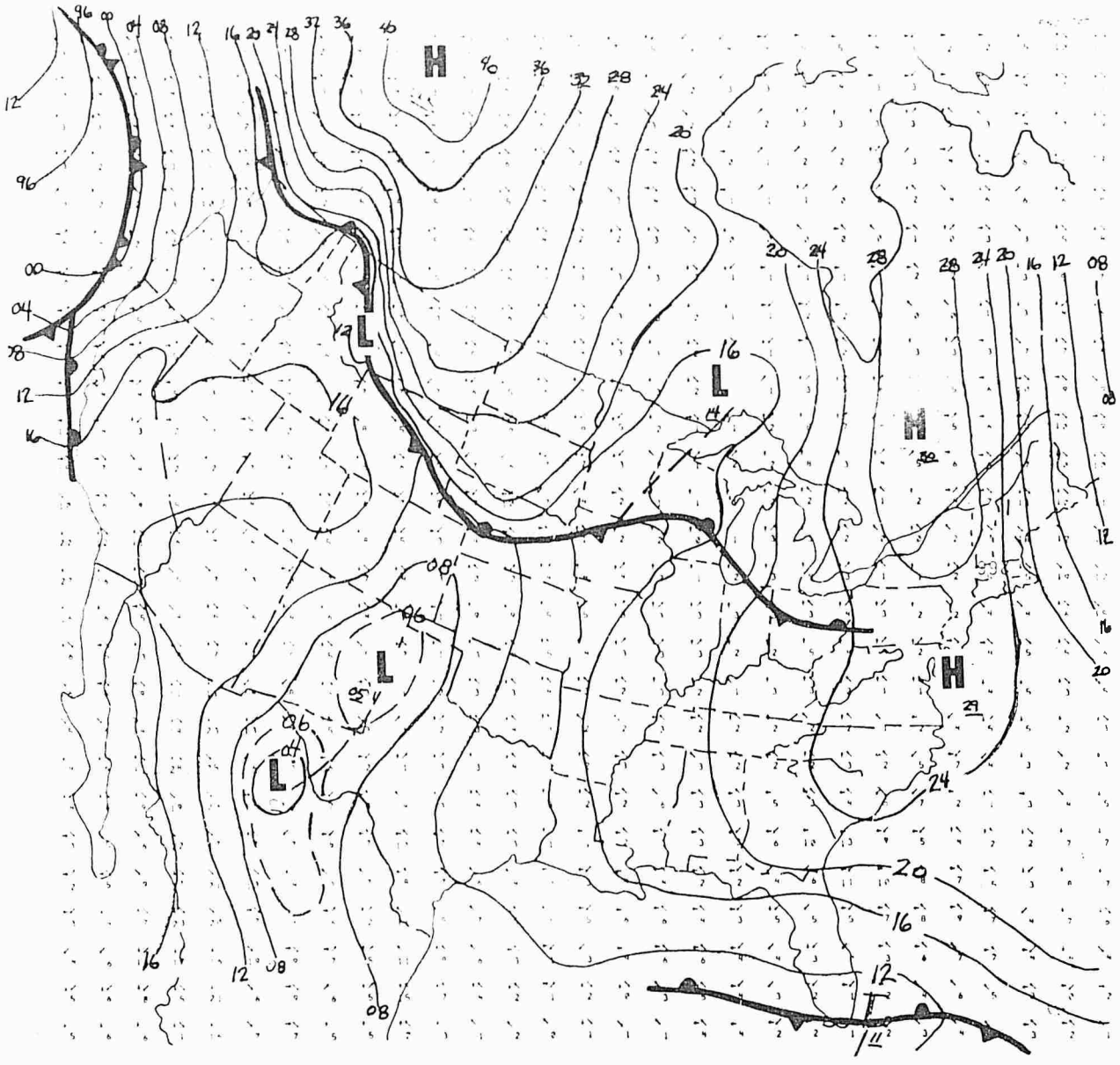

SURFACE ANALYSIS SUPERIMPOSED; WIND SPEEDS IN METERS PER SECOND

FIG. 10 DIAGNOSED 50m WIND FLOW FOR 0000Z 16 JANUARY 1970

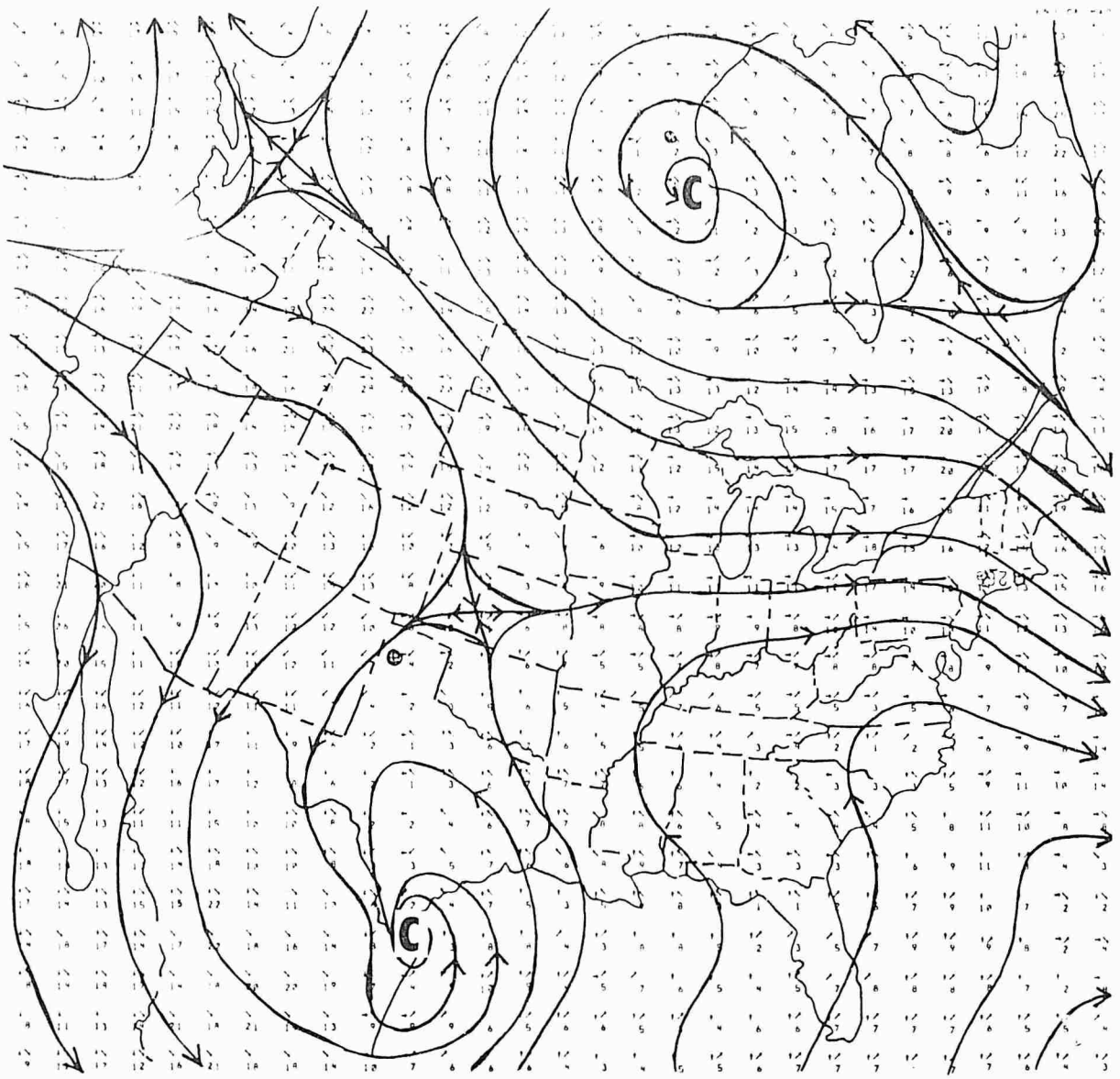

WIND SPEEDS IN METERS PER SECOND

FIG. 11 12 HOUR 1600m WIND FLOW FORECAST
VALID AT 12DDZ 16 JANUARY 1970

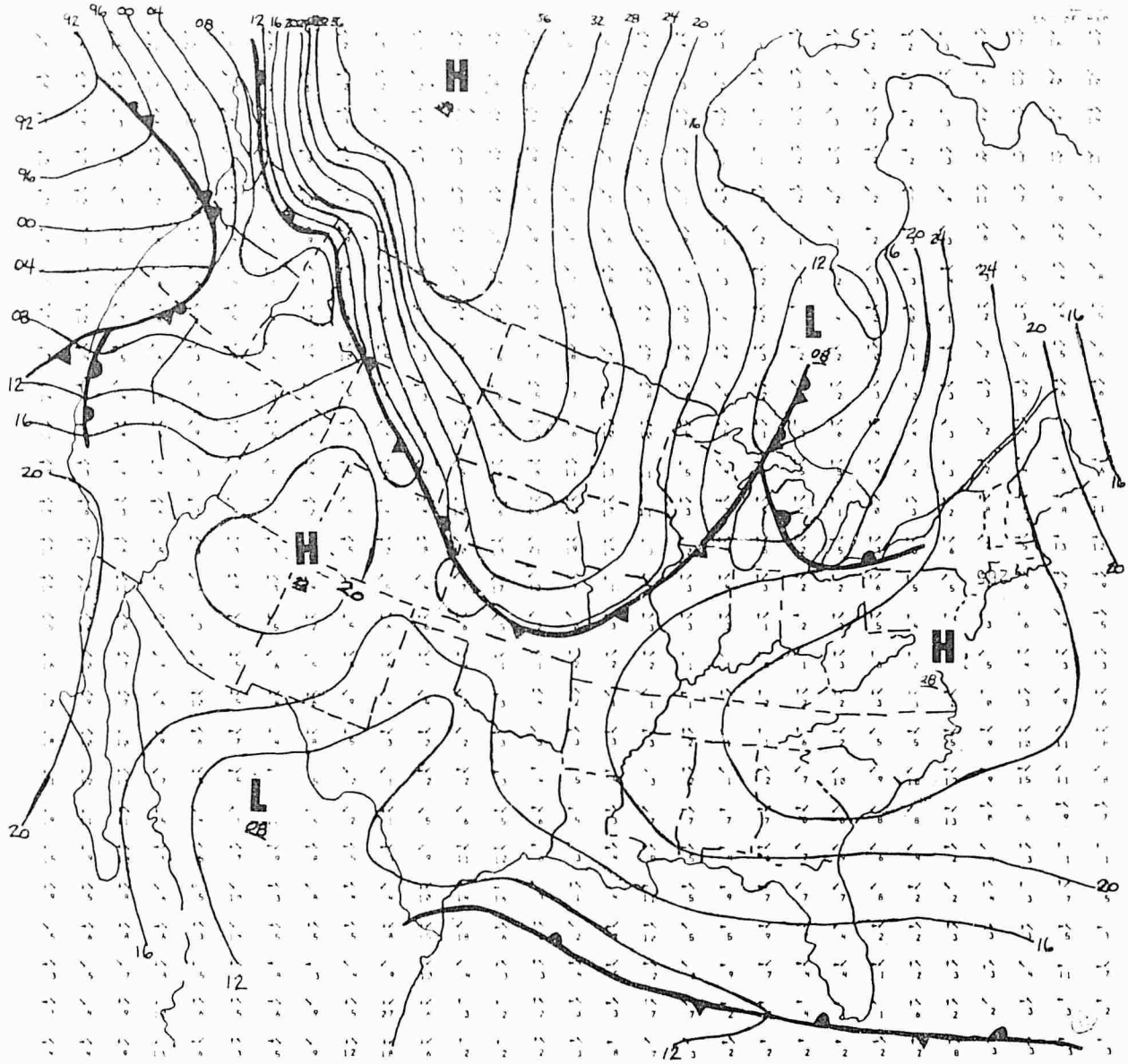

SURFACE ANALYSIS SUPERIMPOSED; WIND SPEEDS IN METERS PER SECOND

FIG. 12 12 HOUR DIAGNOSED 50m WIND FLOW
VALID AT 1200Z 16 JANUARY 1970

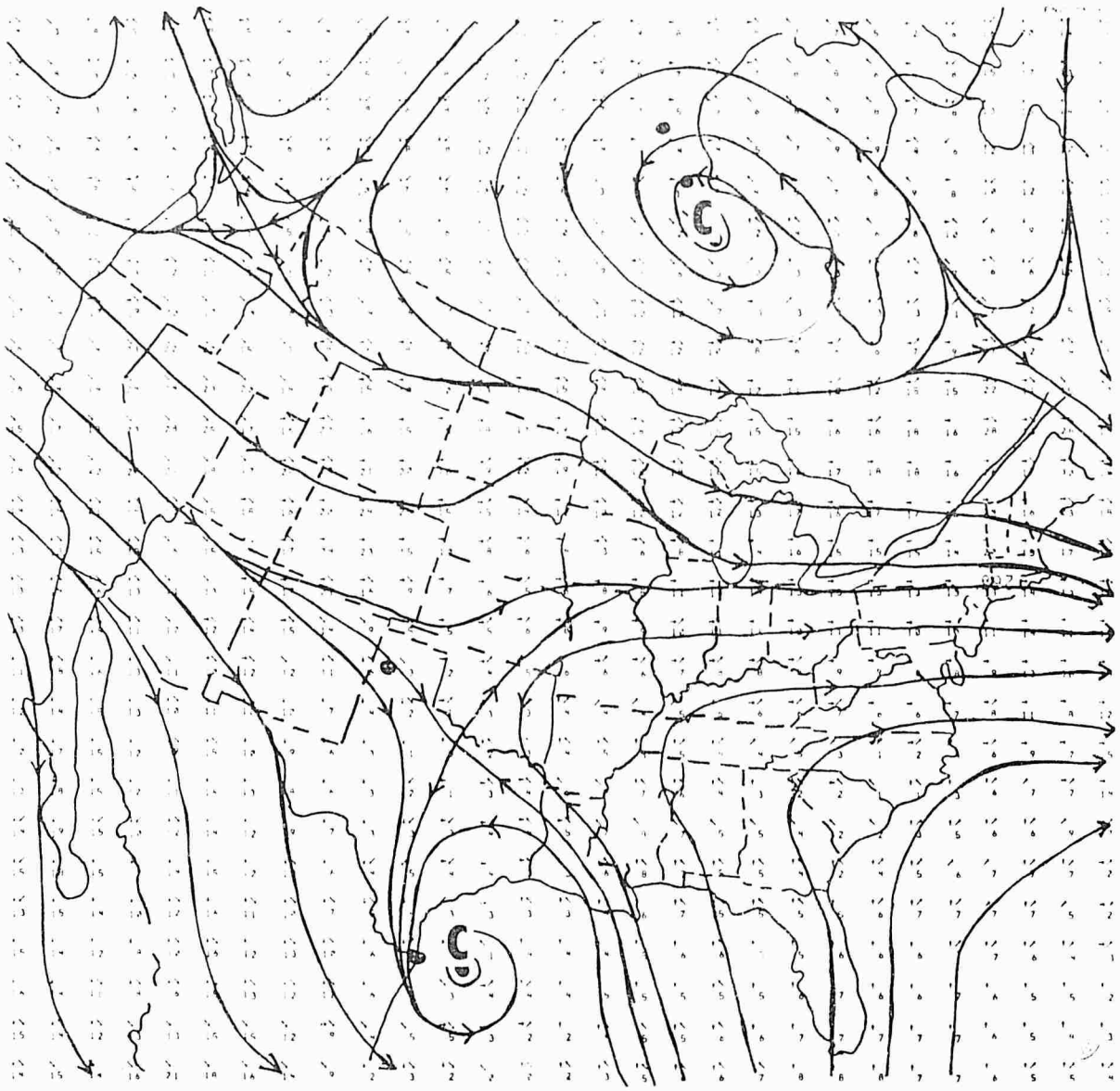

WIND SPEEDS IN METERS PER SECOND

FIG. 13 24 HOUR 1600m WIND FLOW FORECAST
VALID AT 0000Z 17 JANUARY 1970

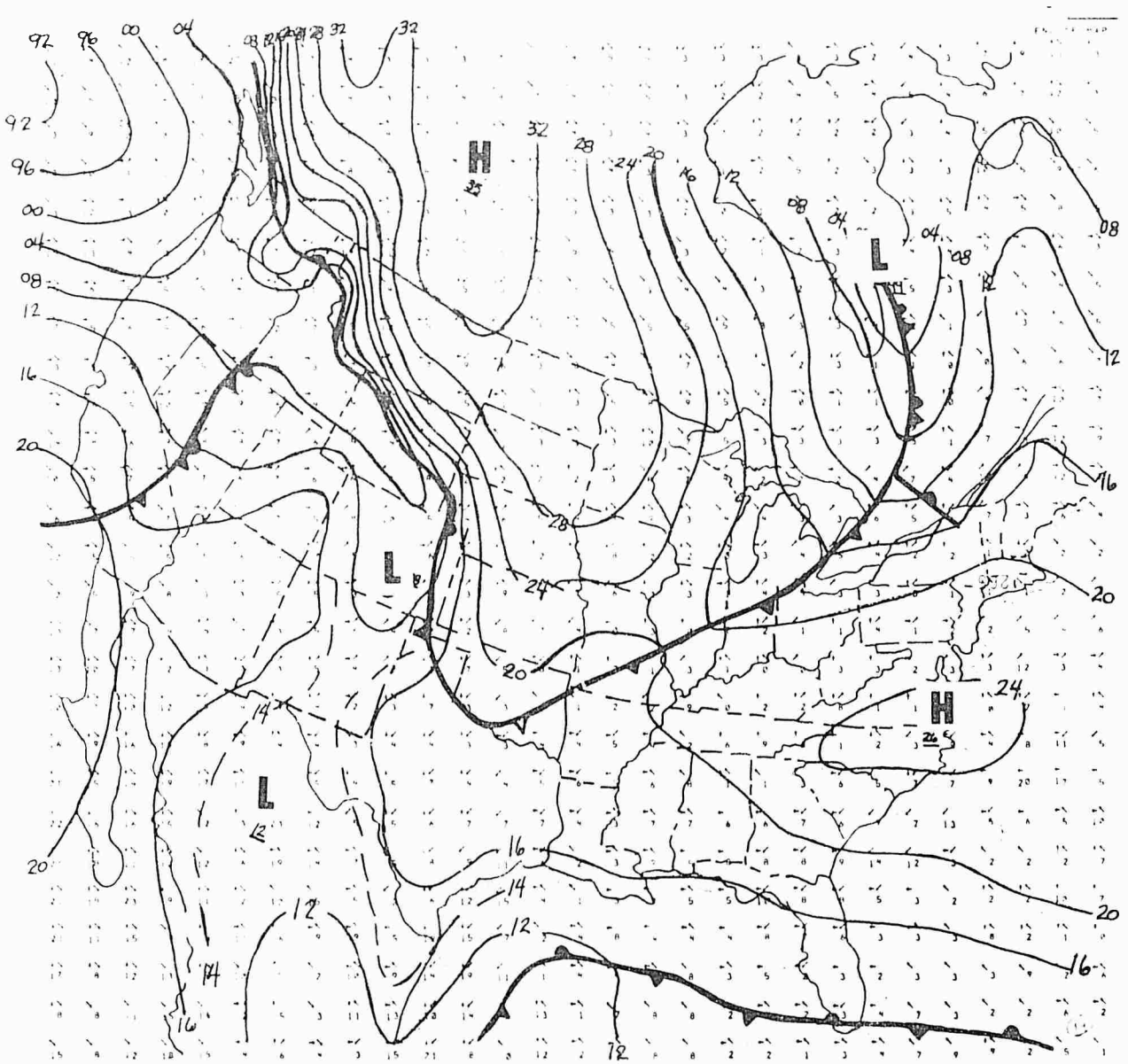

SURFACE ANALYSIS SUPERIMPOSED; WIND SPEEDS IN METERS PER SECOND

FIG. 14 24 HOUR 50m WIND FLOW FORECAST

VALID AT 0000Z 17 JANUARY 1970

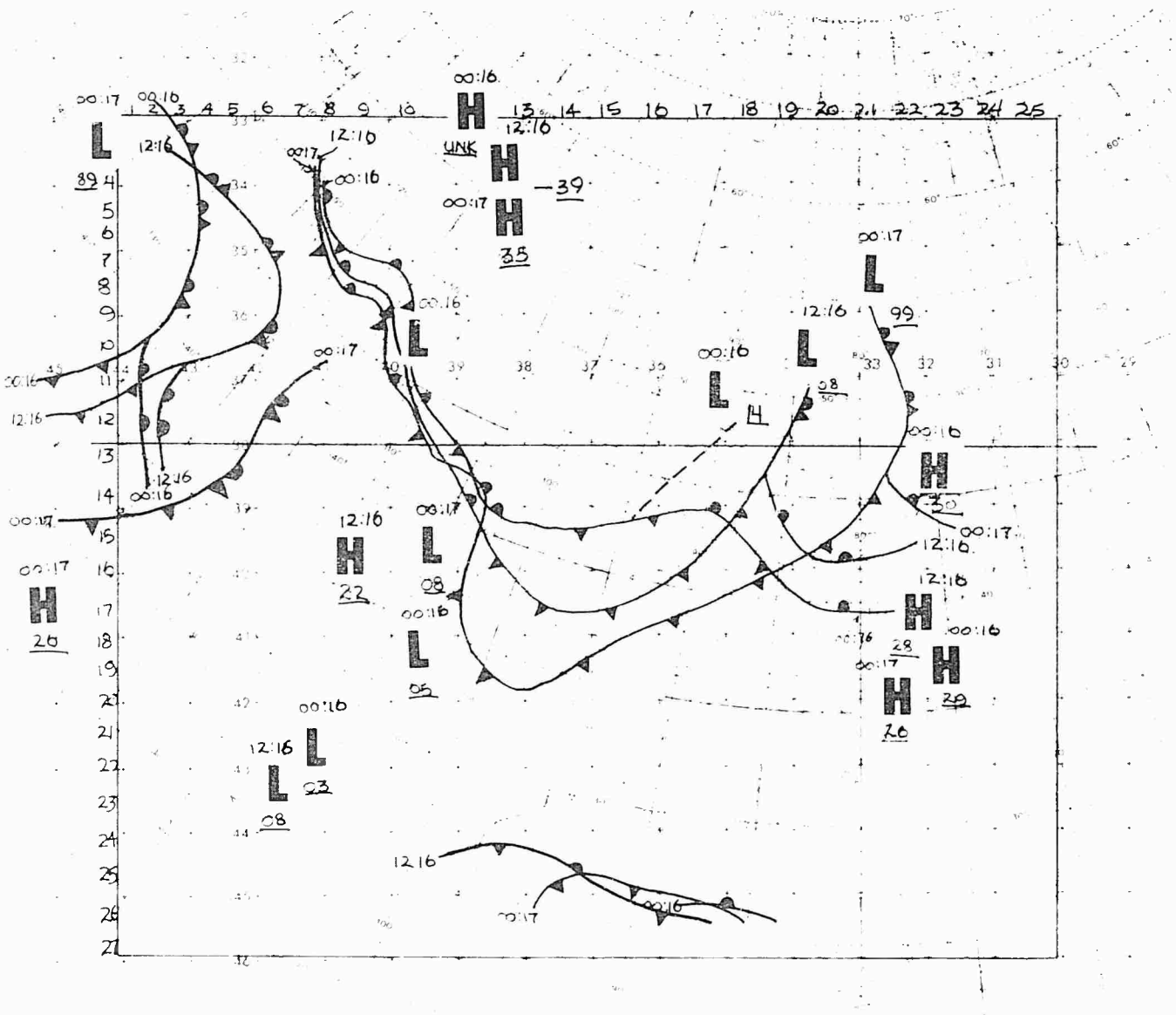

FIG. 15 FRONTAL CONTINUITY CHART FOR 16/0000Z TO 17/0000Z JANUARY 1970

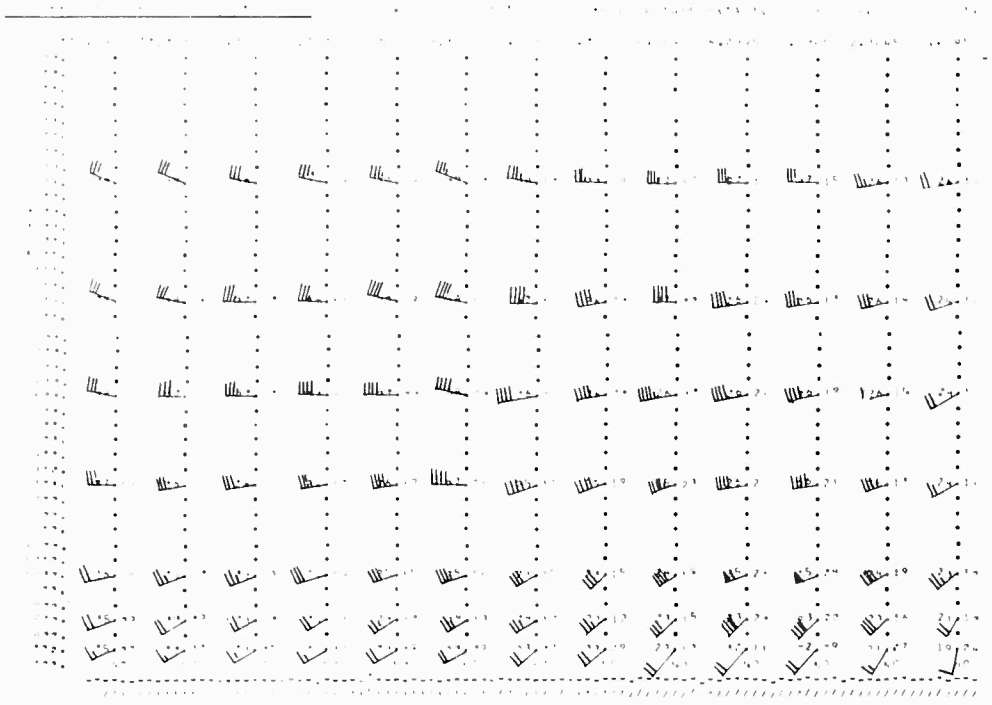

SUBTRACT 45 DEG FROM WIND DIRECTIONS SHOWN
TO OBTAIN TRUE DIRECTIONS.

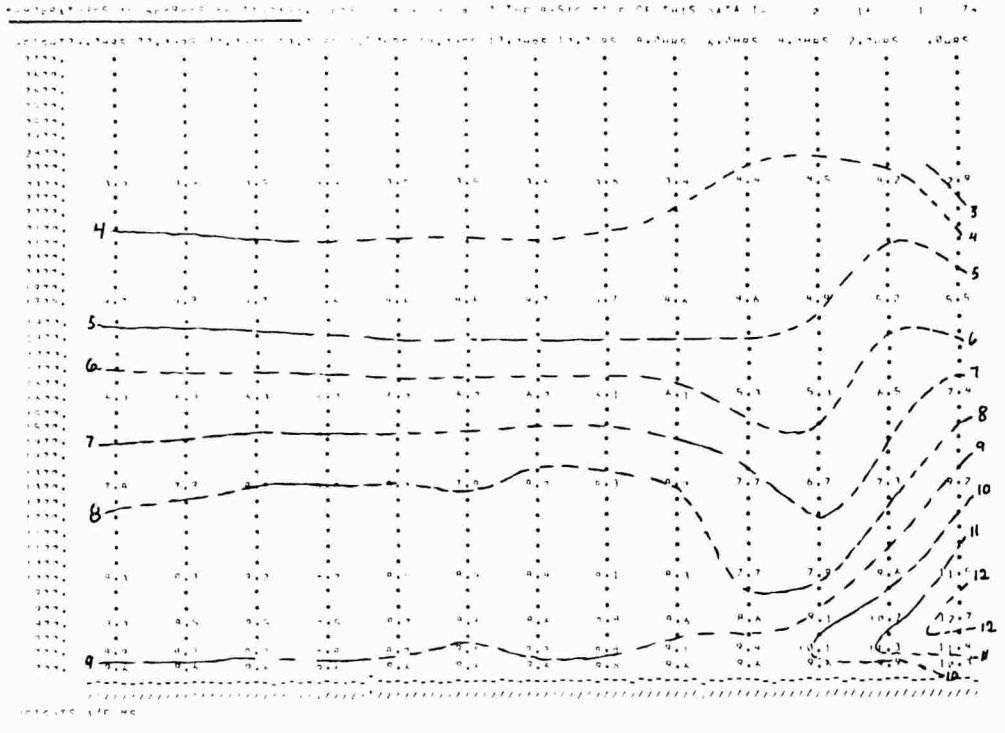

FIG. 16 TIME CROSS-SECTION OF WINDS AND TEMPERATURES FOR MEDFORD, OREGON

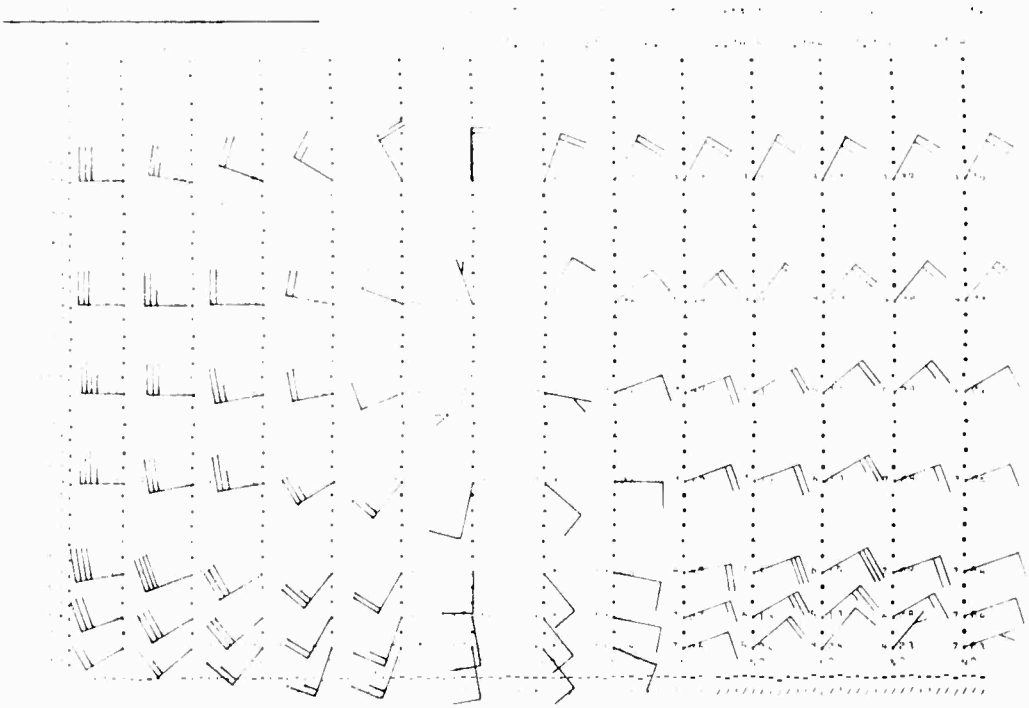

SUBTRACT 25 DEG FROM WIND DIRECTIONS SHOWN
TO OBTAIN TRUE DIRECTIONS.

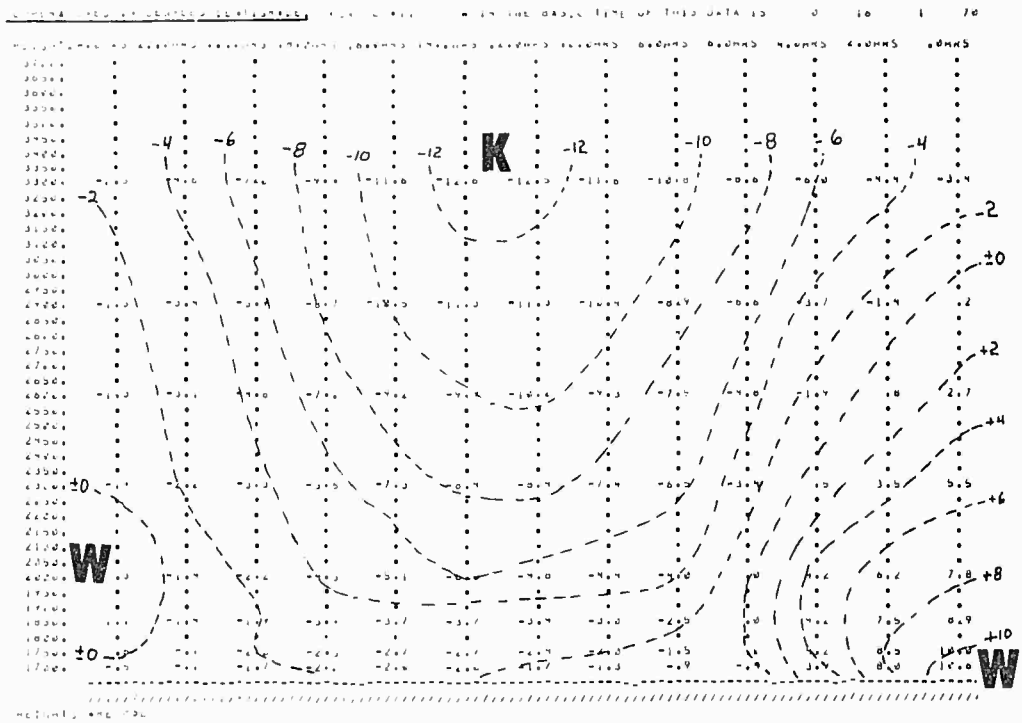

FIG. 17 TIME CROSS-SECTION OF WINDS AND TEMPERATURES FOR LIMON, COLORADO

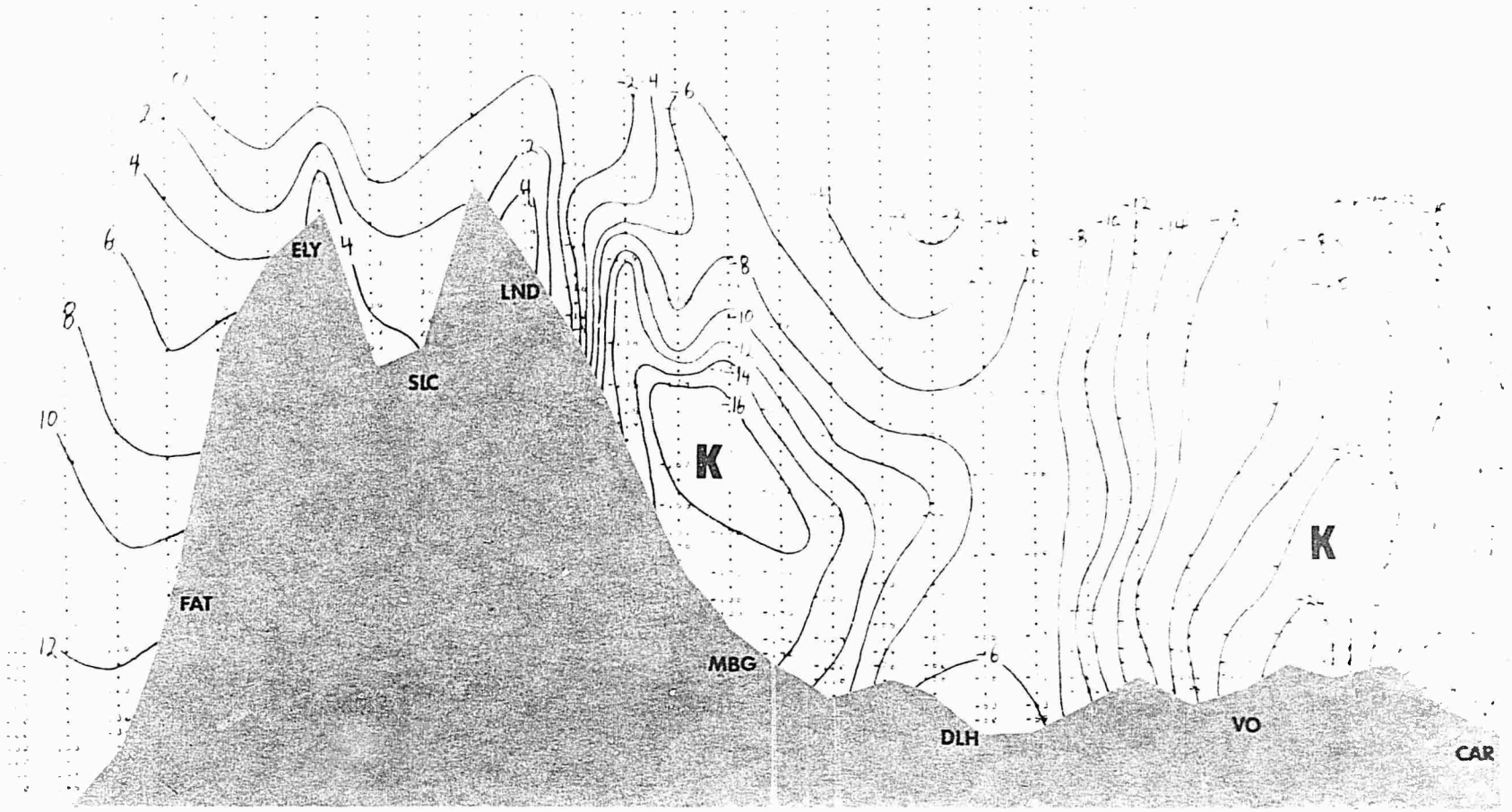

FIG. 18 TEMPERATURE CROSS-SECTION (ROW 11)
VALID 0000Z 16 JANUARY 1970

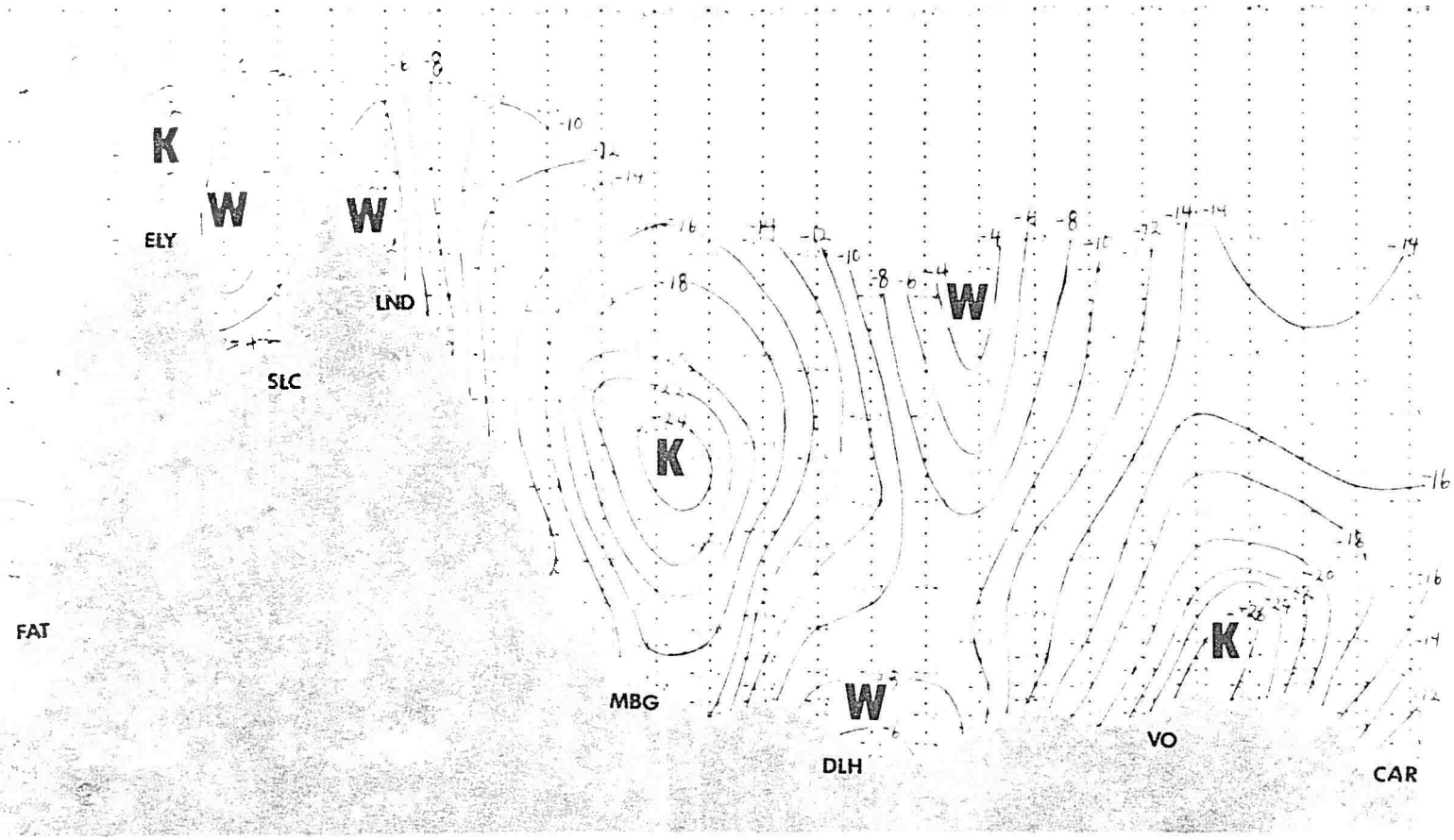

FIG. 15 -- 12-HR FORECAST TEMPERATURE CROSS-SECTION ROW 11
VALID 1200Z 15 JANUARY 1970

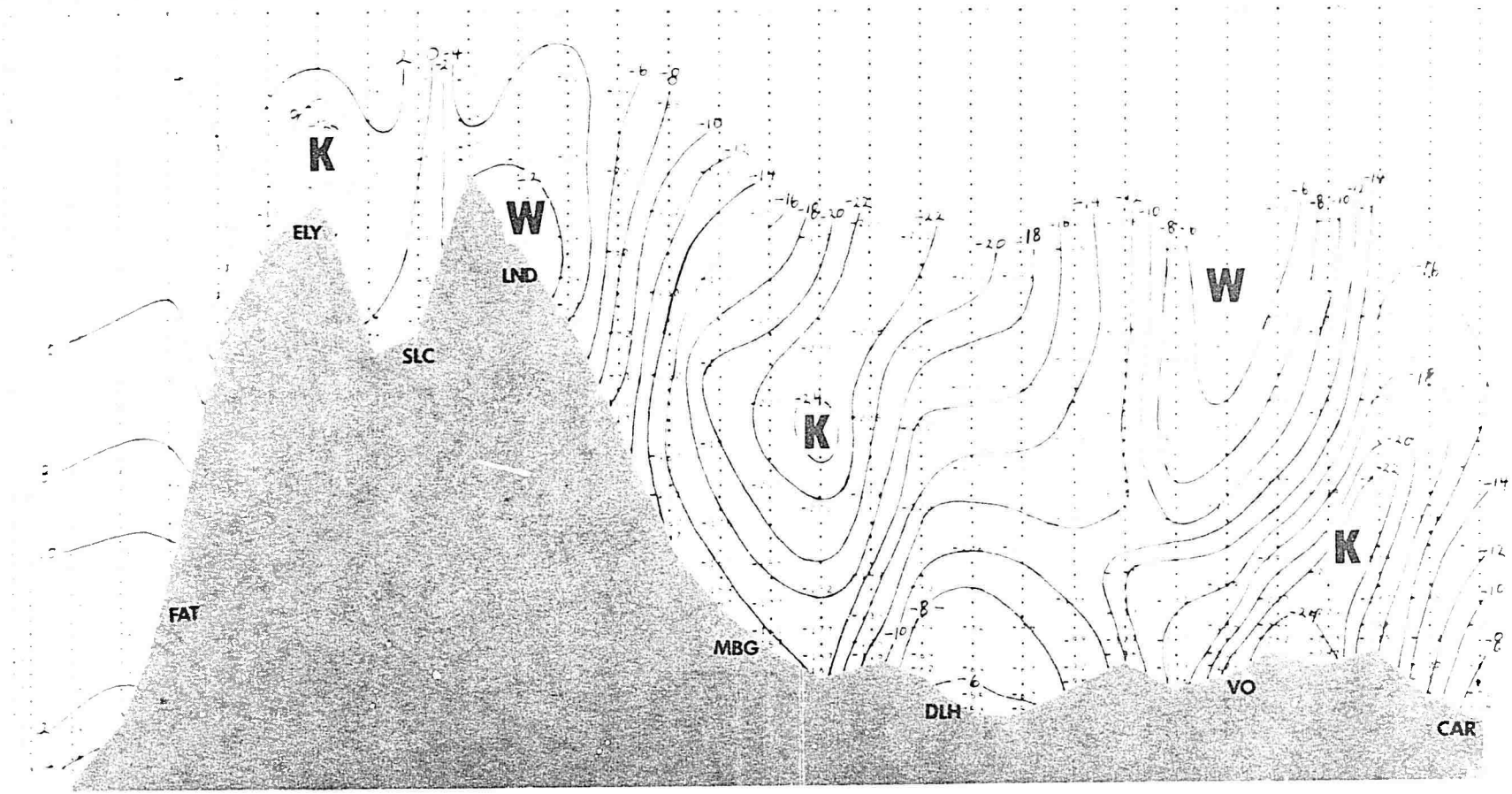

FIG 20 24 HOUR FORECAST TEMPERATURE CROSS-SECTION (ROW 11)
VALID 0000Z 17 JANUARY 1970

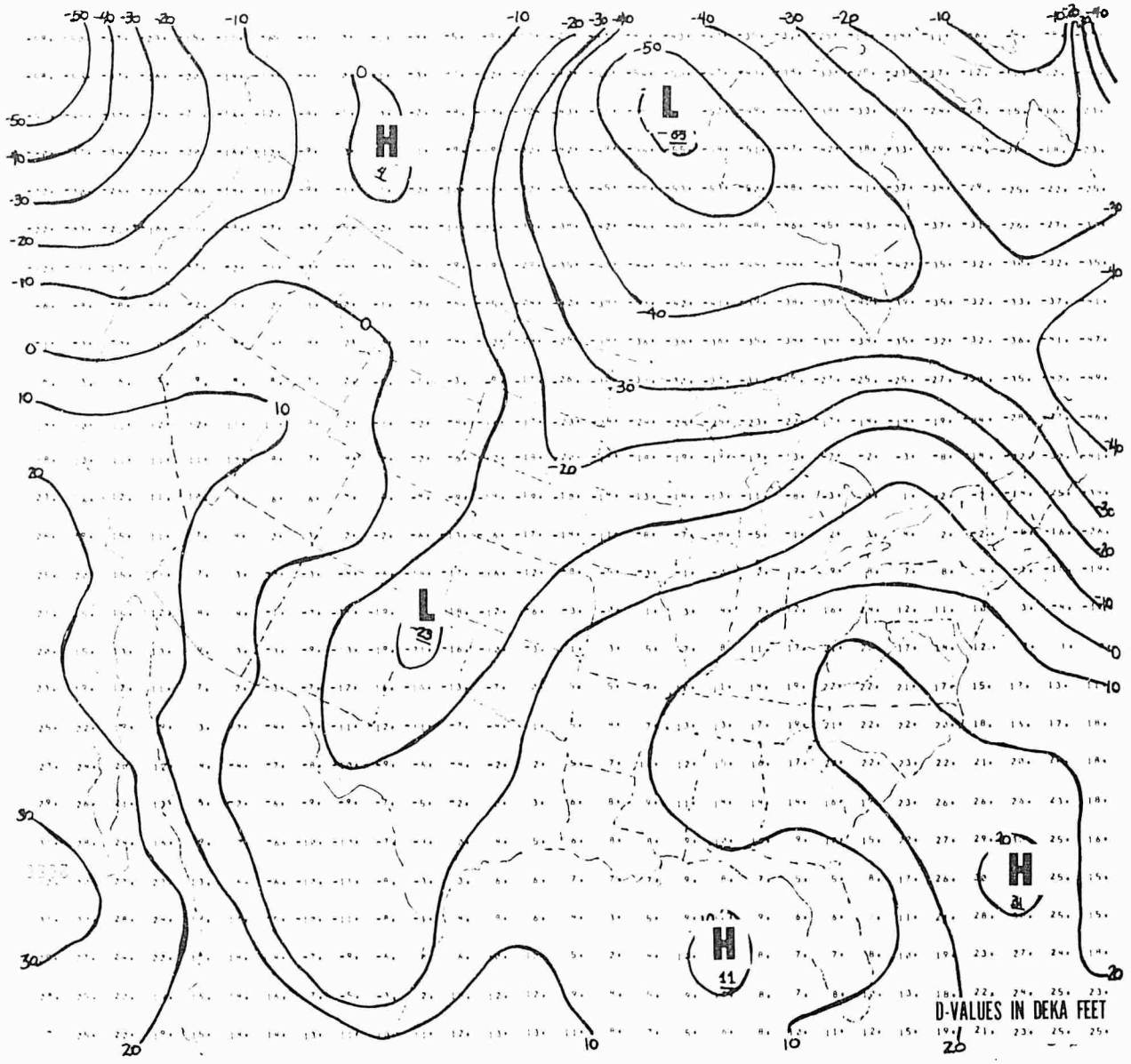

FIG. 21 1600m D-VALUE FIELD AT 0000Z 16 JANUARY 1970

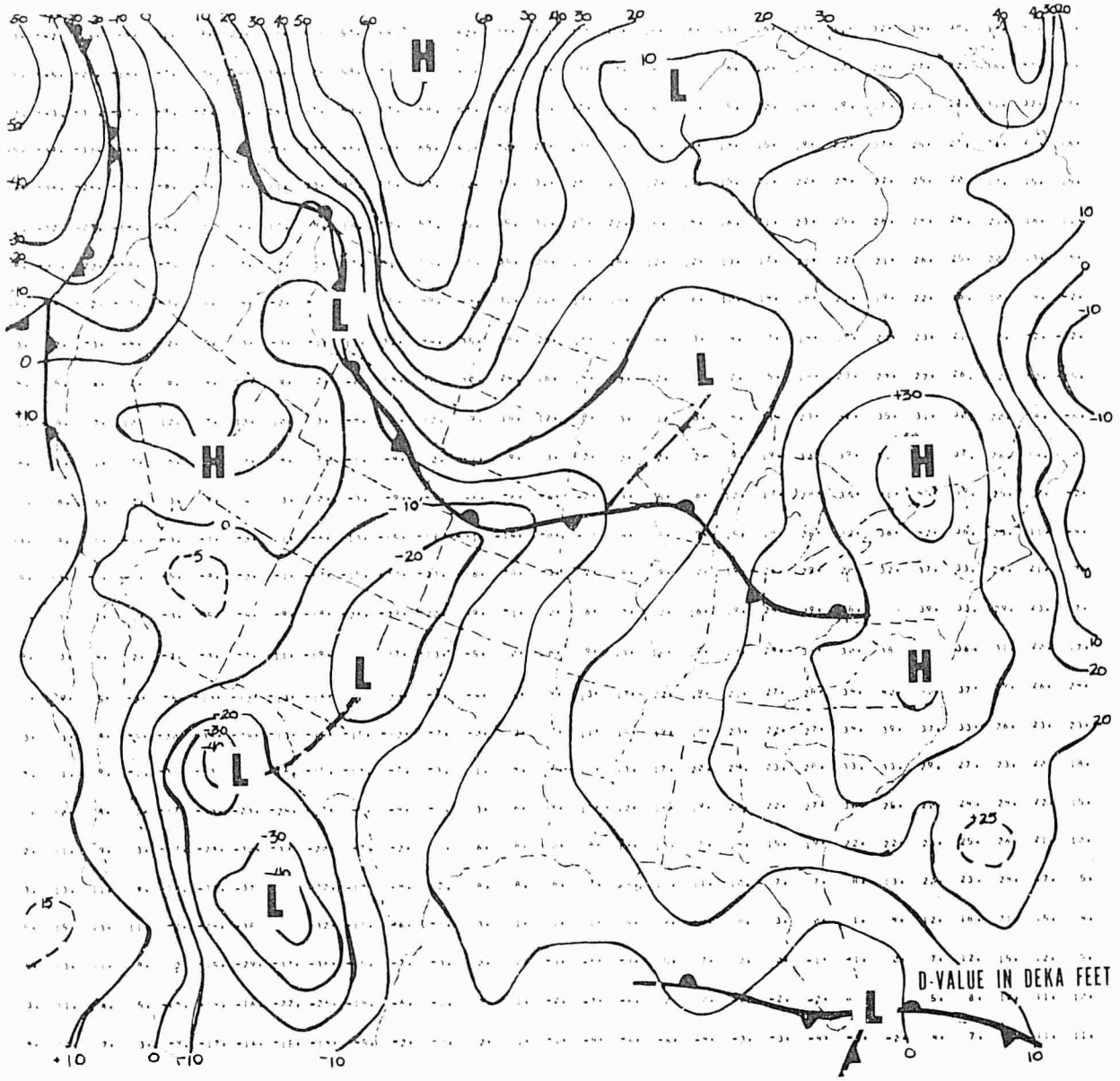

FIG. 22 COMPUTED SURFACE D-VALUE FOR 0000Z 16 JANUARY 1970

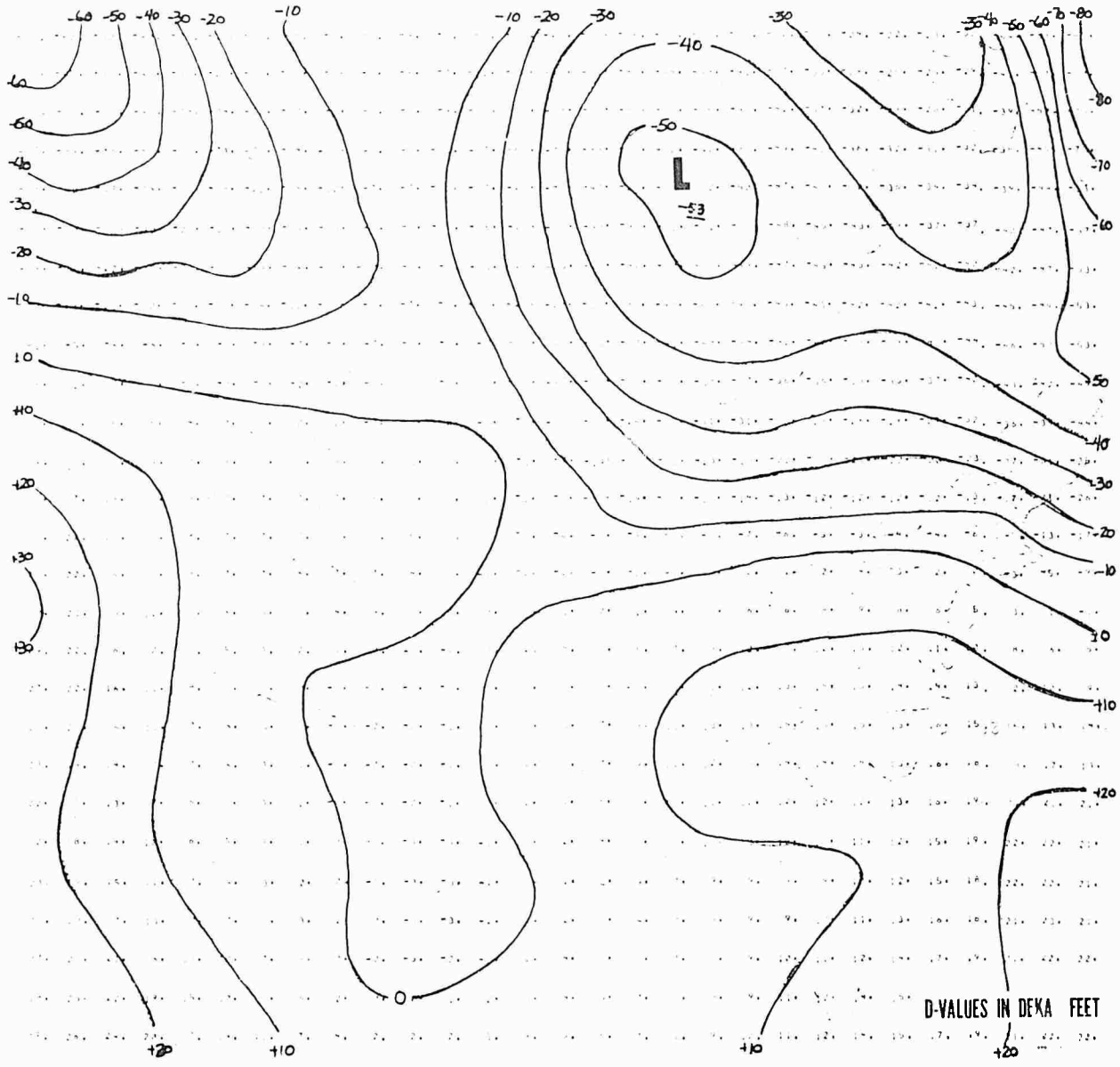

FIG. 23 12 HOUR 1600m D-VALUE FORECAST
VALID AT 1200Z 16 JANUARY 1970

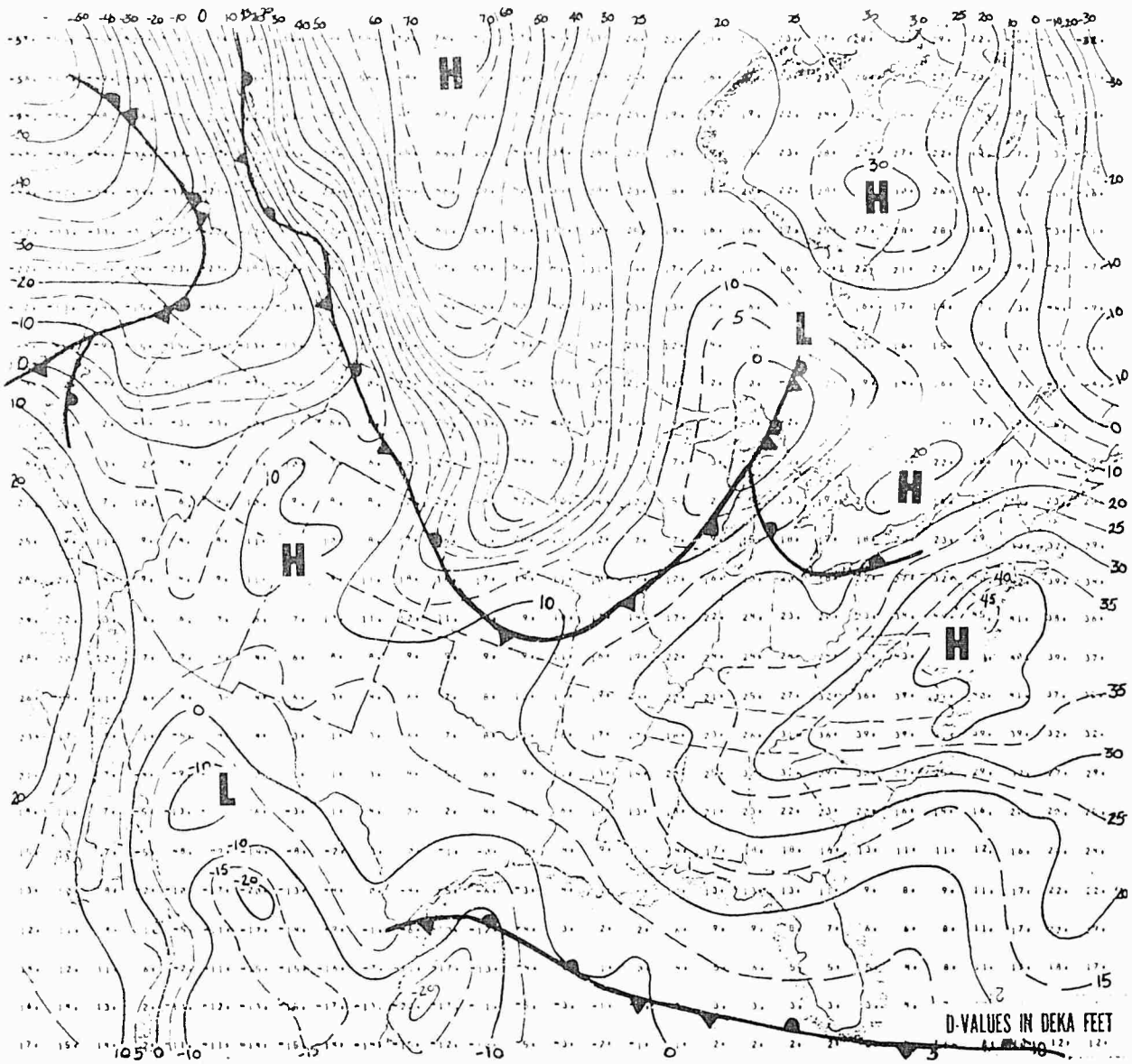

FIG. 24 12 HOUR SURFACE D-VALUE FORECAST
VALID AT 1200Z 16 JANUARY 1970

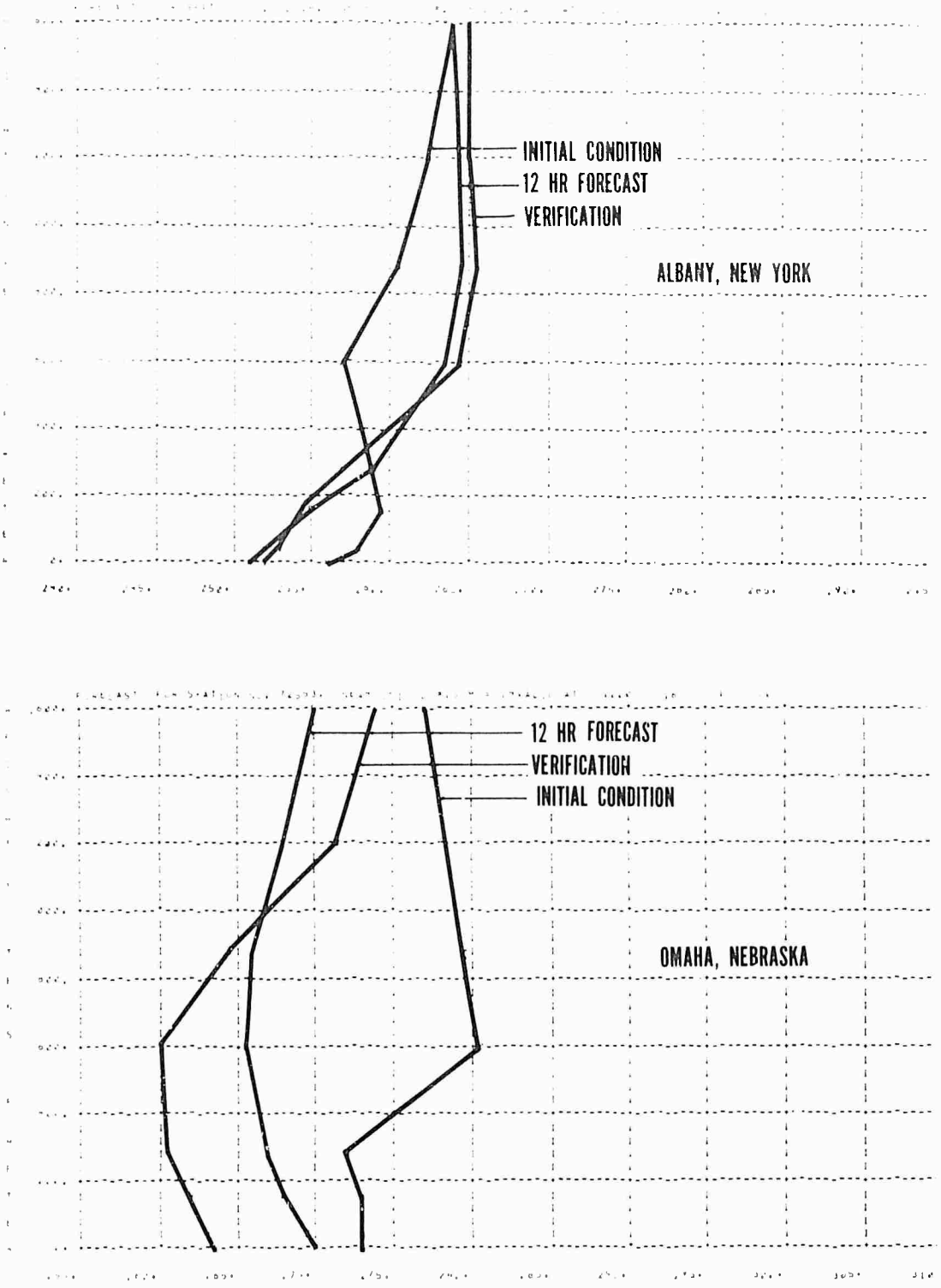

FIG. 25 TEMPERATURE SOUNDINGS FOR ALBANY, NEW YORK AND OMAHA, NEBRASKA

[illegible], [illegible] Planetary Boundary Layer Analysis Model, by Capt [illegible]. [illegible], [illegible] 1966.

[illegible], [illegible] Fog-Stratus Prediction Model, by Capt James Griffin. [illegible], [illegible] 1967.

[illegible], [illegible]: Technique for Analyzing Details in Numerical Weather Analysis, Journal of Applied Meteorology, 3(4), Aug 1964.

[illegible], [illegible]: The Vertical Distribution of Wind in a Baroclinic Adiabatic Atmosphere Boundary Layer, Dept of Meteorology, Pennsylvania State University, 1963 (unpublished).

[illegible], [illegible], [illegible] Covey, and [illegible] Merryman: Design of Experimental Meteorological Simulators, Third Quarterly Progress Report, 1 June to 31 Aug 1966, Signal Corps Contract DA-36-039 SC-74975. Dept of Oceanography and Meteorology, The A and M College of Texas, College Station, Texas.

[illegible], [illegible]: The Sea Breeze as a Function of the Prevailing Synoptic Situation, Journal of the Atmospheric Sciences, 19(3), Dept [illegible], 491-497.

[illegible], _____ _____: A Numerical Model of the Atmospheric Boundary Layer, Journal of Geophysical Research, 68(4), Feb 1963, 1169-1183.

[illegible], [illegible]: 'A Physical Low-Cloud Prediction Model.' L.G. Hanscom Field: 438L System Program Office, Electronics Systems Division, Oct 1965.

[illegible], _____ _____: A Physical-Numerical Model for the Prediction of Synoptic-Scale Low Cloudiness, Monthly Weather Review, 95(5), May 1967, 281-282.

[illegible], [illegible]: The Saturation Adjustment in Numerical Modelling of Fog, Journal of the Atmospheric Sciences, 20(5), Sept 1963, 476-478.

[illegible], [illegible], [illegible] Cooley, and [illegible] Lewburg: Preliminary Investigations of Numerical Models for the Short-Period Prediction of Wind, Temperature and Moisture in the Atmospheric Boundary Layer, Final Report 7047, U.S. Weather Bureau Contract CWB-10368. The Travelers Research Center, Inc., Hartford Conn., 1963.

AFGWCTM 70-2 THE AFGWC MACRO-SCALE UPPER AIR ANALYSIS MODEL, Major August L. Shumbera, 15 Mar 70, 2[illegible] pages.

AFGWCTM 70-4 THE AFGWC MACRO-SCALE BAROCLINIC PREDICTION MODEL, Capt Kenneth J. Palucci, 15 Mar 70, 14 pages, AD 709[illegible].

AFGWCTM 70-5 AFGWC BOUNDARY LAYER MODEL, [illegible],

1 Apr 70, [illegible].

(CONTINUED FROM PAGE ii)

UNCLASSIFIED

Security Classification

DOCUMENT CONTROL DATA - R & D

(Security classification of title, body of abstract and indexing annotation must be entered when the overall report is classified)

1. ORIGINATING ACTIVITY (Corporate author)
Air Force Global Weather Central
Offutt Air Force Base, Nebraska, 68113

2a. REPORT SECURITY CLASSIFICATION
UNCLASSIFIED

2b. GROUP

3. REPORT TITLE
AFGWC PLANETARY LAYER MODEL

4. DESCRIPTIVE NOTES (Type of report and inclusive dates)

5. AUTHOR(S) (First name, middle initial, last name)
Lt Col Kenneth D. Hadeen

6. REPORT DATE	7a. TOTAL NO. OF PAGES	7b. NO. OF REFS
1 April 1970	59	11

8a. CONTRACT OR GRANT NO	9a. ORIGINATOR'S REPORT NUMBER(S)
b. PROJECT NO	AFGWC TM 70-5
c.	9b. OTHER REPORT NO(S) (Any other numbers that may be assigned this report)
d.	

10. DISTRIBUTION STATEMENT

This document has been approved for public release and sale; its distribution is unlimited.

11. SUPPLEMENTARY NOTES	12. SPONSORING MILITARY ACTIVITY
	Air Force Global Weather Central Offutt Air Force Base, Nebraska 68113

13. ABSTRACT A limited area seven layer physical-numerical model for the lower tropospheric region (surface-1600m) is described. The grid interval is half that of the standard numerical weather prediction grid used in the hemispheric, free atmospheric operational model at the Air Force Global Weather Central (AFGWC). This model is an integral part of the complete AFGWC meso-scale (sub-synoptic) numerical analysis and prediction system. This model provides greater horizontal and vertical resolution in both the numerical analyses and numerical forecasts. It is used to predict the more detailed smaller scale atmospheric perturbations which are important in specifying sensible weather elements.

Important features of this boundary layer model include; a completely automated objective numerical analysis of input data: the transport of heat and moisture by three dimensional wind flow (including terrain and frictionally induced vertical motions). Latent heat exchange in water substance phase changes; and eddy flux of heat and water vapor.

Input data are conventional synoptic surface and upper air reports. Other prediction models provide horizontal wind components at the upper boundary and an estimate of cloudiness above the boundary layer region. Forecasts for the lower boundary and surface layer are empirically derived. Despite some approximations which broadly simplify the real planetary boundary layer processes, operational use indicates the model is capable of producing detailed forecasts out to 24 hours. A winter case study is discussed.

DD FORM 1 NOV 65 1473

UNCLASSIFIED

Security Classification

14 KEY WORDS	LINK A		LINK B		LINK C	
	ROLE	WT	ROLE	WT	ROLE	WT
Numerical Weather Prediction						
Meteorological Data Processing						
Atmospheric Boundary Layer						
Meso-scale analyses						
Planetary Boundary Layer						
Temperature Forecasting						
Sub-synoptic wind prognoses						
Vertical Motion Forecasts						